Energy & Environmental Science

ROYAL SOCIETY OF CHEMISTRY

ANALYSIS

View Article Online
View Journal | View Issue

Cite this: *Energy Environ. Sci.*, 2025, **18**, 6854

Closing the carbon cycle: challenges and opportunities of CO_2 electrolyser designs in light of cross-industrial CO_2 source-sink matching in the European landscape†

Muhammad Tayyab, ‡[b] Maximiliane Dreis, ‡[a] Dennis Blaudszun,‡[a] Kevinjeorjios Pellumbi, ‡[a] Urbain Nzotcha, ‡[b] Hermann Tempel, ‡[b] Muhammad Qaiser Masood,[a] Henning Weinrich, [b] Sebastian Stießel,[a] Kai junge Puring,[a] Rüdiger-A. Eichel *[bcd] and Ulf-Peter Apfel *[ae]

The defossilisation of the chemical industry is a critical milestone in achieving climate-friendly and sustainable production routes. In this regard, CO_2-electrolysis technologies have emerged as a foundational element of carbon capture and utilisation (CCU) technologies, facilitating the valorisation of CO_2-emissions as a source of valuable synthons. However, there are still fundamental questions that must be addressed. These include identifying the most promising CO_2 point sources, determining the maturity level of the different reactor designs, and identifying which target product has the highest drop-in market potential. The objective of this study is to establish a comprehensive carbon source-sink roadmap for today and in the future (*i.e.* 2050), with a particular emphasis on the European context. In this article, we integrate the current and projected demand for products and building blocks derived from CO_2-electrolysis and CO_2-emissions from industrial sectors with inherent CO_2-emissions. Additionally, we explore the role of direct air capture in the future. Strengthened by a statistical analysis of over 5000 publications relating to CO_2-electroreduction covering both low- and high-temperature electrolysis for three different product classes (CO, formic acid as well as ethylene/ethanol) conclusions on the most probable employment scenarios for each technology are drawn. We believe that this analysis will serve to stimulate discourse and the establishment of CO_2-to-X value chains among academic and industrial collaborators, while concurrently furnishing the community with a roadmap of the requisite issues that must be addressed, promoting finally better data reporting and standardisation of metrics.

Received 2nd January 2025,
Accepted 23rd April 2025

DOI: 10.1039/d4ee06204c

rsc.li/ees

Broader context

Over the past decade, CO_2 electrolysis has emerged as a promising route to produce chemical building blocks using renewable electricity. However, key questions remain—what CO_2 sources are viable, which products should be prioritized, and how ready the technology is across Europe. This work places CO_2 electrolysis in a broader techno-economic and environmental context to clarify its potential across various industrial sectors. By analysing market needs and emission trends through 2050, we identify how unavoidable CO_2 emissions from industries like the cement, pulp/paper, and glass industries, along with direct air capture, can form a complementary network to establish an electrified CO_2-based chemical production. Accompanied by a statistical analysis of over 5000 publications we reveal the currently achieved metrics of different reactor types, configurations, and target products, helping to define integration scenarios for implementing CO_2 electrolysis at scale. Simultaneously, these scenarios stress the need for dedicated infrastructure and consistent data reporting to drive faster innovation and meaningful comparison across systems. By aligning technical development with infrastructure planning and policy frameworks, this work outlines a clear path for accelerating CO_2 electrolysis and advancing a more sustainable, electrified chemical industry.

[a] *Fraunhofer Institute for Environmental, Safety and Energy Technology UMSICHT, Oberhausen, Germany. E-mail: peter.apfel@umsicht.fraunhofer.de*
[b] *Forschungszentrum Jülich, Institute of Energy Technologies – Fundamental Electrochemistry (IET-1), Jülich, Germany*
[c] *RWTH Aachen University, Institute of Physical Chemistry, Aachen, Germany*
[d] *RWTH Aachen University, Faculty of Mechanical Engineering, Aachen, Germany*
[e] *Ruhr University Bochum, Inorganic Chemistry I, Bochum, Germany. E-mail: ulf.apfel@rub.de*

† Electronic supplementary information (ESI) available. See DOI: https://doi.org/10.1039/d4ee06204c

‡ These Authors contributed equally to the work.

1. Introduction

The critical issue of climate change, along with the need to meet climate targets, has recently created an immense environmental, societal and political impetus to defossilise the chemical industry.[1,2]

While complete decoupling from fossil fuels and mitigation of associated CO_2-emissions remains a major challenge for industrial sectors, alternative pathways for recycling CO_2-emissions have emerged. In an effort to close the carbon cycle, carbon capture and utilisation (CCU) technologies have come to the forefront as a means of converting emitted CO_2 into value-added carbon products and synthons, with the goal of minimizing the environmental impact of industrial sectors with inherently elevated CO_2-emissions.[3–6] Among these novel CCU pathways, CO_2-electrolysis takes a pivotal role towards the creation of more sustainable chemical production routes.[7–10] Powered directly by renewable energy sources, these emerging technologies can convert CO_2 both in its gaseous and captured form to a variety of carbon products such as carbon monoxide (CO), formic acid (HCOOH), ethylene (C_2H_4), ethanol (C_2H_5OH) as well as lower alcohols and acids.[7,11,12] Most interestingly, CO_2-electrolysers can be directly coupled to existing infrastructure both in a centralised and decentralised manner, being modularly adaptable, depending on the application scenario.[13] These integration capabilities will enable the electrification of the chemical industry, which is currently the missing link for linking the key industrial sectors of heat, energy, transport and production. Enabling this sector coupling through power-to-X (P2X) technology would enable sustainable and climate-neutral production in the chemical industry.[14,15] However, despite the milestones achieved in recent years, the feasibility of CO_2-electrolysis as a drop-in solution has yet to be demonstrated.[16]

While CO_2 electroreduction (CO_2R) has made exponential progress in recent years at the lab scale and in start-up efforts, the following critical questions remain regarding the practical implementation of the technology.[17–20] Namely:

I. Which industrial sectors are most promising for such carbon source-sink matching for scaled-up scenarios?

II. Which sector could provide the envisioned impact of CO_2-electrolysis in the EU market, both in the present (2023-standpoint) and in the future?

III. What is the current level of maturity and drop-in compatibility for each carbon-product produced *via* CO_2-electrolysis?

With CO_2 electrolysers available in a variety of configurations, it remains difficult to clearly understand the advantages/disadvantages and industrial applicability of different reactor configurations, especially when considering the variety of possible CO_2R products and their specific downstream requirements.[21,22] To address these above questions, two frameworks are developed for matching CO_2 electrolysis to the industrial context in the current study:

1. Cross-industrial source-sink matching: identifies the most relevant point sources and CO_2R products for coupling scenarios.

2. Product-to-electrolyser matching: evaluates the performance of various CO_2R products across reported cell configurations, highlighting key achievements, trends, and areas for improvement.

This work aims to bridge the gap between academic reviews on CO_2R progress and industrial point sources. The frameworks consider both current CO_2 emissions and market demands, as well as projections for 2050, offering a long-term perspective on the potential of CO_2-electrolysis.

In addition, the developed technical review aims to be the "missing" link between comprehensive academic reviews of progress for the various CO_2R products, reactors,[21,23–25] and the industrial point-sources. Our study highlights opportunities, challenges, and areas for improvement in large-scale source-electrolyser integration while emphasizing the importance of standardised data reporting in scientific publications.

2. Methodology

Aiming to understand the application scheme of CO_2 electrolysis and harmoniously achieve the target of industrial source-sink matching, this study is divided into three categories:

I. CO_2 sources identification: The identification of CO_2 emission sources and their associated availability for further electrochemical upcycling.

II. Demand projection: The demand projection for the different CO_2R carbon products is also included the market identification.

III. Technological review: The current technical maturity of the CO_2R field depending on the employed electrolyser architecture and target compounds. The three most reported routes for CO_2 electrolysis are analysed in the current study are as follows:

a. CO_2-to-CO and syngas, encompassing their production both *via* low-temperature (25–80 °C) and high-temperature solid-oxide (500–850 °C) electrolysers.

b. CO_2-to-formate/formic acid.

c. CO_2-to-C_2 products (ethylene and ethanol).

Specifically, regarding the followed strategy in the first two levels of endeavour, attention was paid upon industrial CO_2 point sources characterised by unavoidable CO_2 emissions[26] either due to: (i) societal needs (ii) inherent process-related CO_2 emissions, *e.g.* cement production or (iii) associated with energy intensive processes which are difficult to electrify.

To compare CO_2 availability and market demand, three value chains categories are established. These three targeted product classes (CO, formate/formic acid, and ethylene as well as ethanol) are converted into CO_2 equivalents to create a source-sink match. The source-sink match is projected based on current values as well as projected values for the 2050 market in Europe. Here growth values according to market studies within a scope of 5–10 years are taken into account and extrapolated to 2050. Moreover, two scenarios are deduced by either: (i) extrapolating the data directly as is, being the higher boundary of the projected CO_2R product demand, and (ii)

compensation of certain product values chains, which will interfere/compete with each other in a defossilised future, *e.g.* synthesis of ethylene through the methanol-to-olefins route (MtO), constituting the lower boundary of our analysis. Finally, CO_2 demand is calculated based on the specific kilogram of CO_2 required per kilogram of product, combined with market study projections for product demand.

Moving to the level of technological maturity, a Scifinder search report was generated by carefully selecting keywords (Table S1 and Fig. S1 and S2, ESI†) appearing in various publications, including more than 5000 academic reports.

In the initial refinement process, model-only reports and reports using only lab-scale H-type cells were excluded. The final step was to define a list of key performance indicators (KPIs) to assess maturity from an industrial perspective for each CO_2R product and cell route. The defined KPIs are as follows:

I. Faradaic efficiency (FE).

II. Current density.

III. Electrode area.

IV. Operation time.

Since in the case of high-temperature CO_2R often a FE_{CO} value close to 100% is reached, the specified KPIs set here include the cell voltage, as well as the corresponding current density, the electrode area, and finally the operation time. It is crucial for this study that the selected publication clearly mentions these KPIs either in the manuscript or in the ESI.† It also focuses on selecting the current density achieved at the highest FE value among the different reports in the present study. While this selection may not directly reflect the highest value, we believe it provides a better overview of the threshold for selective generation of each value-added product. In particular, the implementation of this analysis already leads to a significant reduction in the number of validated publications (close to 1000) (Fig. S1, ESI†).

A complete overview of the data collected for the box plots discussed here can also be found in the attached tables in the ESI.† Similarly, since the herein developed technical overview majorly focuses on the reactor configuration, reports that did not fully explain the employed reactor configuration or provide only a descriptive schematic/photograph were also excluded. Compared to previous literature reports,[21,23,24,26] we believe that this methodology provides a more comprehensive overview on the state of the CO_2R field across all its possible modes of operation and reactor configurations. This allows us to better understand in retrospect what is the differentiating factor for the observed performance, *i.e.*, catalyst, electrode, reactor design or the operational conditions. Nevertheless, it is paramount to emphasise the importance of proper data presentation to enable the production of more robust and fruitful reports on the state of the CO_2R field.

Finally, combining both the market and technical maturity data in the latter part of this report, a critical perspective on the most promising CO_2-value chains and reactor types are provided, depending on the needs and characteristics of the different point sources (Fig. 1).

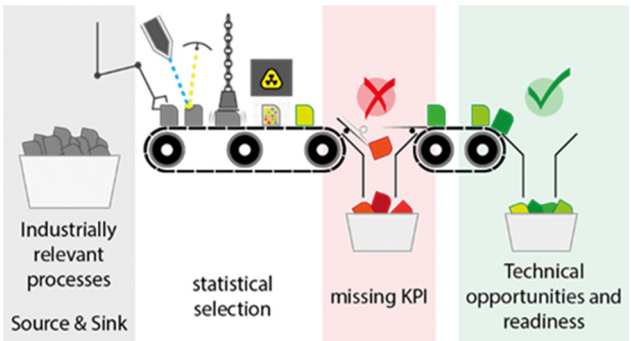

Fig. 1 Schematic representation of the followed methodology within the presented statistical analysis.

3. Identification of source-sink match

The amount of CO_2 emissions from industrial operations must be equal to the growth rate of the plants, trees, and microbes used in fermentation processes to defossilise the chemical products. Such synchronization does, however, present the problem of human and plant competition for land use. A methodical approach is essential for evaluating the feasibility of biogenic feedstocks. The use of primary biogenic carbon sources is limited by the continuous struggle with food production, especially given the world's constantly growing population. Finding substitute sources that don't disrupt food supply systems is necessary because of this restriction.

Although biogenic waste and residual materials offer a potential solution to this issue, it is crucial to remember that their quantity and quality might not be enough to satisfy the needs of the chemical manufacturing industries of the present and the future. Therefore, it is essential to investigate alternative plant-based feedstocks that can complement present biogenic carbon sources while also making sure that sustainable industrial practices are upheld, and land-use conflicts are kept to a minimum.

In addition to bio-based materials and recycling, the chemical industry's sole additional carbon source is CO_2,[27] which can be obtained through direct air capture (DAC) or point source emissions. Although DAC technologies have gained significant traction in recent years, they have yet to achieve a fully competitive maturity level from an economic standpoint when compared to direct point-source capture.[28] In contrast, the use of point sources for CO_2 electrolysis and hence value-added chemical production will only be sustainable if the CO_2 from the source can be clarified for carbon neutrality.[27]

At present, various entities, including political entities, commercial enterprises, and non-profit associations, are actively engaged in the discourse surrounding the term "recycled or secondary-used carbon" for chemical production within the context of national carbon management systems (NCMS). The primary motivation for this discourse is the recognition of the significantly superior environmental carbon footprint exhibited by recycled or secondary-used carbon when compared to that of primary fossil carbon.

Moreover, unavoidable process-related CO_2 emissions represent a potential opportunity for the sector to engage in synergies with the chemical industry. This is due to the ease with which such emissions can be managed and the spatial synergies that exist between sources and locations, such as refineries, and existing and future carbon demand. An example for this possible sector coupling is the direct use of process gases as a carbon source from the steel production as demonstrated *e.g.* in the Carbon2Chem® project.[29]

Potential value chains from CO_2 point sources and DAC to various products in the chemical industry are depicted in Fig. 2A. The utilisation of CO_2-electrolyser technologies enables the direct pathways (highlighted in red) to be realised for the production of essential building blocks (*i.e.*, CO/syngas), bulk chemicals (ethanol, and prospectively methanol), monomers (ethylene), and fine chemicals (*i.e.*, alcohols and formic acid). In addition, further downstream processing enables indirect access to refined fuels, monomer/polymer and fine chemical products. These include the following processes:

I. Long chain hydrocarbons and alcohols *via* Fischer–Tropsch routes or ethers (*i.e.*, dimethyl-ether-DME, polyoxymethylene dimethyl ethers-PODE, methyl *tert*-butyl-ether-MTBE),

II. Formaldehyde and ethylene/propylene *via* methanol synthesis, methanol oxidation and MtO.

Thus, electrochemical processes can not only supplement the current chemical industry with crucial building blocks, but also provide novel options from direct CO_2-utilisation, which previously required long process chains (*i.e.*, CO_2-to-Ethylene). Furthermore, formic acid can be used as a proton source or CO building block in carbonylation reactions.[30] This allows to use formic acid as an alternative for CO gas which cannot be easily transported over larger distances due to its toxicity.

To comprehend the availability of CO_2 from various point sources, including unavoidable and energy-intensive processes that cannot be easily directly electrified, emissions in Europe were analysed based on two extrapolation scenarios from 2022 to 2050. These scenarios included a business-as-usual scenario as well as a progressive CO_2 emission scenario (Fig. S3–S5, ESI†). Herein, we focused on industrial sectors with significant point source CO_2 emission, being glass production, waste incineration, paper and pulp, and cement production. Subsequently, the data is then matched with market data for carbon monoxide, ethylene, methanol, ethanol, formaldehyde, and formic acid, which are key chemicals. The annual tonnages for each product were converted into CO_2 equivalents (Fig. S6 and S7, ESI†) with the consideration of a carbon capture efficiency of 80% and a maximum utilisation value of 70% across the complete spectrum of possible products and envisioned value-added chain. These values were inspired by previous reports on the global deployment of e-fuels and e-chemicals by Galimova and co-workers, taking into account that demand and supply within the presented value added chain are unlikely to align perfectly across all sites due to location, timing mismatches, and other factors influencing suitability (Fig S4, ESI†).[31] Moreover, two further potentially interesting industrial point sources that were not considered in our sink-source matching, include steel fabrication as well as biodigesters. Both examples could provide CO_2 at an elevated purity and act as potential point sources at different scales and locations, as steel production is more centralised while biodigesters could be characterised as a more ubiquitous and decentralised source of CO_2. In these cases, it is important here to note that both of these point sources are not often discussed in the context of CO_2 electrolysis either due to technology shifts or existing knowledge gaps. Specifically, in the case of steel, there has recently been a gradual shift towards the establishment of green steel both in the Chinese and European markets, instead of process coupling with CCU routes.[32–35] On the other hand, biodigesters often generate a mixture of CO_2 and CH_4, where most research is focusing on the generation of methane through microbial electrolysis and thus further investigation of their source-sink matching potential.[36–39]

In case of the methanol market, the shares for ethylene (*via* the MtO route) and formaldehyde are omitted due to their separate denomination. The market demands are projected to 2050 according to reported compounded average growth rates (CAGR) and supplemented to a sensitivity analysis with a ± 20% variation on the CAGR (Fig. 2B). A further overview of our methodology and drawn conclusions in regard to the source-sink matching for the different industries and products, alongside the obtained data sets, can be found in the ESI† (Supporting Note S1 and appended tables).

An analysis and comparison of these scenarios on a European basis (Fig. 2C) for 2022 highlights the fundamental contribution of the waste incineration (211 Mt a^{-1}), cement (108 Mt a^{-1}) as well as paper and pulp (79 Mt a^{-1}) industries, due to their high production volume, inherent process related CO_2 emissions, and high energy use. On the contrary, CO_2 emission from the glass industry lies at just 9 Mt a^{-1}. When projected to 2050, it can be expected that a decrease in European population[40] and increased recycling efficiency[41] will drastically reduce the convertible CO_2 emissions from waste incineration to 104 Mt a^{-1}. Accordingly, the projected more energy-efficient production of paper and pulp (63% cut in energy demand)[42] as well as the glass industry (75% cut in energy demand)[43] outweigh the expected growth in demand, ultimately decreasing the projected CO_2 emissions to 36 Mt a^{-1} and 5 Mt a^{-1}, respectively. In contrast, the use of limestone as raw material in the cement industry limits any process improvements in terms of CO_2 emission compared to our 2022 projection. Notably, even with a full electrification/defossilisation of the sector's energy supply, our analysis suggests a slight increase in CO_2 emissions of 1.7 Mt a^{-1} from 2022 to 2050, indicating the crucial need to develop targeted and scalable CCU solutions for this sector.

As of today, the CO_2 equivalent carbon demand for chemical production of CO_2 electrolysis value chains is heavily outweighed by 250% due to the CO_2 emissions from the above point sources. Currently, ethylene and ethanol represent the main markets for CO_2 electrolyser products followed by

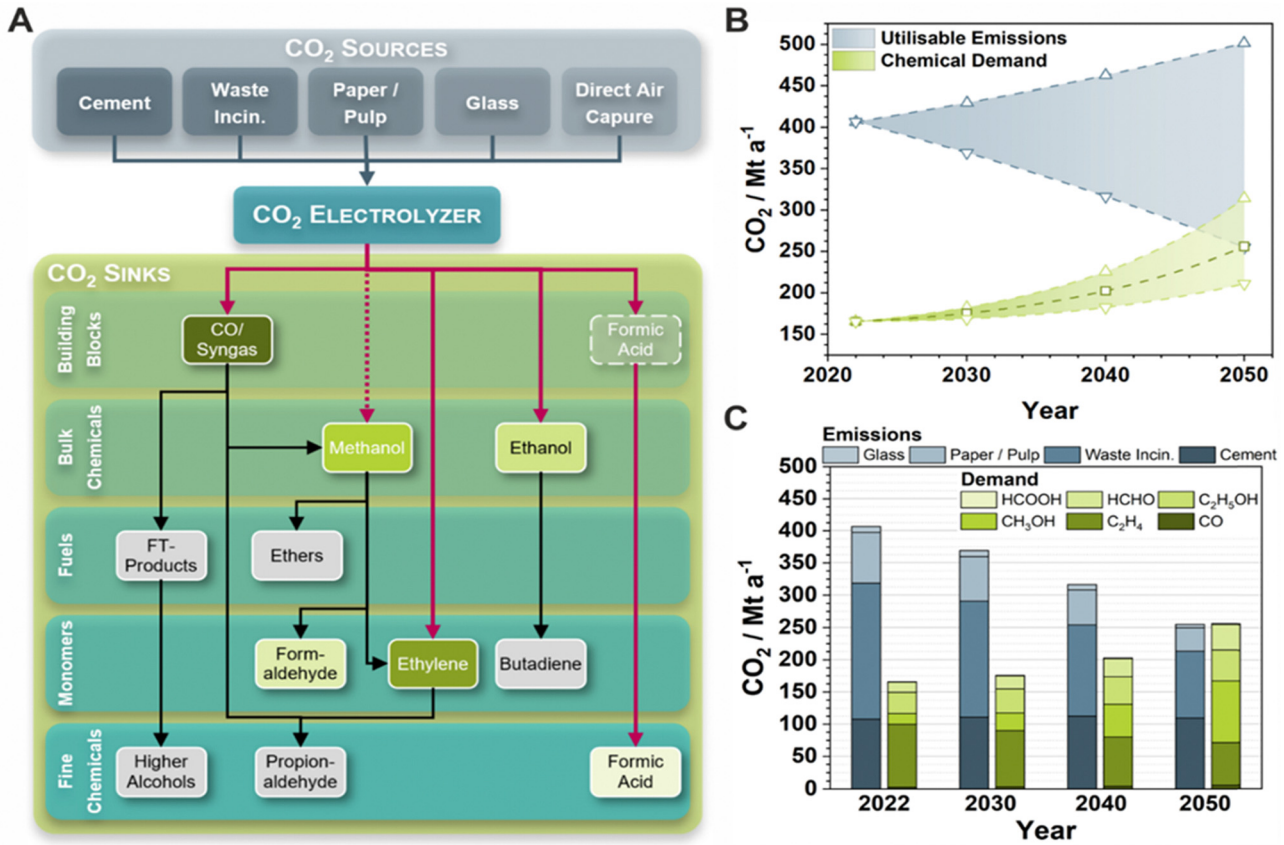

Fig. 2 Analysis of potential CO_2 based value chains with electrochemical pathways highlighted in red (A) and projection of CO_2 emissions from unavoidable CO_2 resources (cement, waste incineration, paper/pulp and glass) as well as demand for key chemical products from CO_2 electrolysis in Europe from 2022 until 2050. (B) depicts the range of the cumulative CO_2 emissions and the chemical demand in CO_2 equivalents. Sinks (green) are estimated based on market studies (square symbols) and are given as a range between progressive (up-pointing triangles) and conservative market developments (bottom-pointing triangles). Sources (grey) are summarised as business as usual (up-pointing triangles) and progressive scenarios (bottom-pointing triangles) emphasizing cuts in CO_2 emissions. (C) highlights the contributions of CO_2 sources (progressive scenarios) and value chains as sinks (base scenario).

methanol and formaldehyde. Carbon monoxide and formic acid are currently considered for niche markets, although typical market studies for carbon monoxide consider its direct pure use, whereas its use as syngas (*i.e.*, as feedstock for methanol or Fischer–Tropsch syntheses) is more pronounced making it one of the key bulk intermediates for the chemical industry.[44] Furthermore, formic acid and carbon monoxide are not sold at stock exchange whereas this might change with the emerging electrolyser technology. While the CO_2 demand (including losses from carbon capture and conversion efficiencies) for the ethylene market is expected to decrease to 66 Mt_{CO_2} a^{-1}, the demand for the methanol market is projected to massively expand to 95 Mt_{CO_2} a^{-1},*i.e.* due to the perspective use of methanol as fuel *e.g.* for maritime transport.[45] Similarly, carbon monoxide,[7,46] ethanol,[47,48] formic acid,[49,50] and formaldehyde[51,52] markets are expected to grow by a factor between 1.5 to 3.4, leading to an overall increase in CO_2 demand for the presented chemical value chains and projected to closely match CO_2 availability from the point source. The current largest DAC projects are on the long-term storage of CO_2 in the form of carbon capture and storage (CCS). With this approach, large companies such as Microsoft in Elsdorf (Germany) and Blackrock in Ector County Texas (US) are attempting to improve their overall carbon footprint and offset difficult-to-avoid Scope 3 emissions.[53–55] Surprisingly, only a few DAC projects are currently focusing on downstream utilisation of CO_2 (CCU). When expecting the improvement of DAC plants in terms of energy requirements and costs, these plants can potentially provide carbon for the chemical sector in the long term. Hence, we conclude that DAC, at least in the medium term, will not be the primary source of CO_2 for the envisioned value-added chain, with the technology gaining further importance as we draw closer to 2050. This time frame denotes that researchers should focus initially on the development and up-scaling of electrolyser systems that are compatible with point sources, developing in parallel through integration concepts between DAC and CO_2 electrolysis.

4. Technological review

4.1. Introduction to cell structures

Given the importance of CO_2 electrolysers for carbon capture and utilisation (CCU), it is noteworthy that this technology is

currently employed in a variety of cell designs.[22,23,56] The choice of such a cell design depends not only on process parameters like temperature or pressure, but also on the target product. For instance, a cell used for a fast screening of new catalyst materials surely will greatly differ from a cell that operates at industrial levels and requires a stable operation over long periods of time[57–59] Additionally, different target products require different chemical conditions and environments, which can be provided more easily by certain types of cells compared to others.

In the context of high-temperature electrolysis (HT), existing fuel cell designs were adapted to facilitate operation in reverse mode.[60] Conversely, low-temperature CO_2 electrolysers (LT) drew inspiration from proton-exchange membrane (PEM) and alkali fuel cells, along with chlorine–alkaline electrolysis.[61] In accordance with the classification system outlined in recent literature,[23] the objective was to categorize cell designs according to their structural characteristics. Specifically, the arrangement of electrodes, membranes, as well as gas and electrolyte flow. A comprehensive review of the extant literature has revealed the presence of specific cell types, including electrolysers employed for direct carbon utilisation or high-temperature electrolysis (Fig. 2).

At operating temperatures exceeding 600 °C, high temperature CO_2 electrolysis is being performed in solid oxide electrolyser cells (SOECs) to generate CO or syngas.[62,63] These cells employ a solid-oxide based electrolyte to separate the two electrodes.[64] At the cathode CO_2 is reduced to CO generating O^2—ions, which traverse the oxide electrolyte, at these elevated temperatures, forming O_2 at the anode. Notably, in some cases, the SOEC cathode is also referred to as the fuel electrode, with the anode being noted as the oxygen electrode due to the ability of SOECs to also reversibly act as fuel cells, generating energy from different feedstocks.[61,65] Currently SOECs can be classified into following three main cell structures:[66]

I. Planar.
II. Tubular.
III. Flat tubular.

In a planar SOEC (Fig. 3i), the catalytic layers (CLs) are applied directly to a support material, which can be either the solid electrolyte or one of the electrodes to form a flat/planar cell. During operation, the cathode can be supplied with either pure or humidified CO_2, as well as a mixture of CO_2 and a safety gas.[67,68] The planar cell can be designed in different shapes, such as rectangle, button, or disk, with the latter two often indicating smaller cell sizes. The simplicity of the single-cell planar design offers advantages such as easy manufacturing and stackability.[63,66]

Tubular SOECs (Fig. 3ii), are in comparison more complex in their design. Here, the cathode is built as a seamless tube

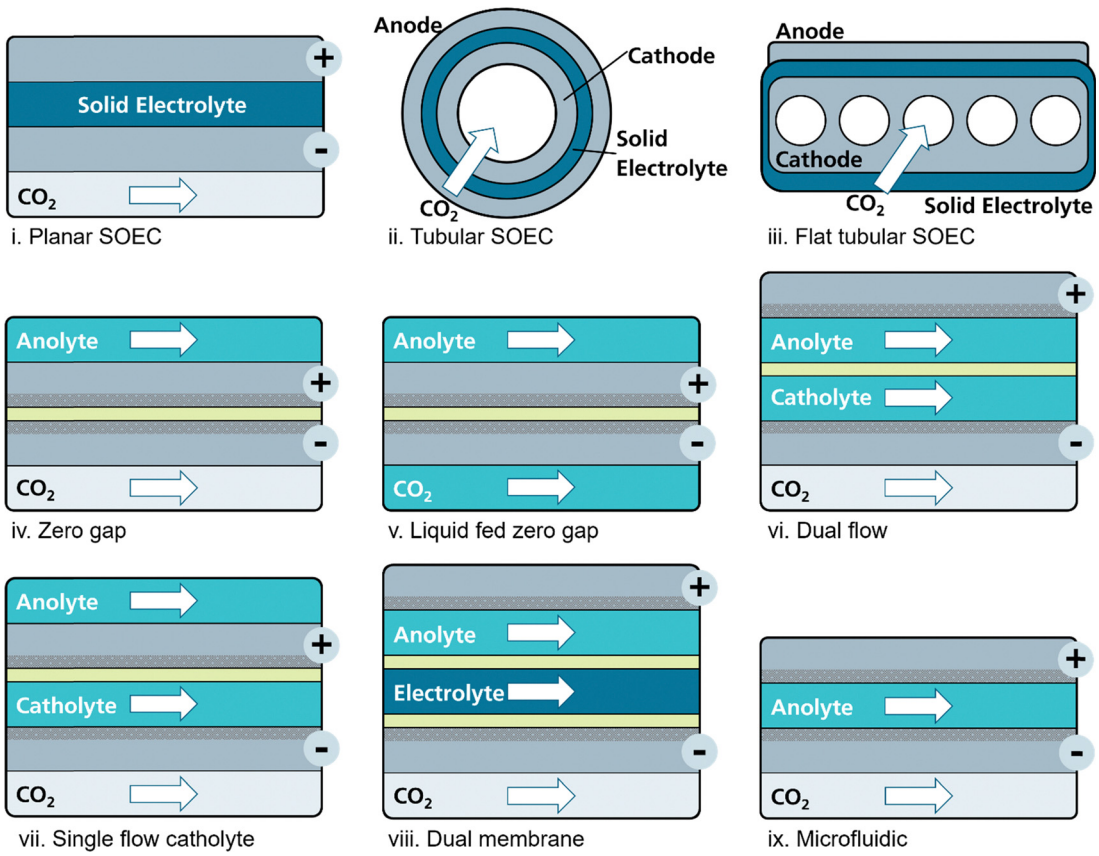

Fig. 3 Schematic representation of the analysed reactor layouts for the electrochemical reduction of CO_2. (i)–(iii) Reactor designs used in high temperature electrolysis; (iv)–(ix) Reactor designs used in low temperature electrolysis.

coated with a layer of solid electrolyte and an anode layer on top. CO_2 is directly supplied through the tubular cathode, while the anode is typically exposed to ambient air. Compared to planar cells, this cell design offers improved thermal stability and easier sealing but exhibits lower volumetric conversion rates.[69] Research on smaller cells, often referred to as microtubular cells, is addressing the issue of lower volumetric conversion rates, as the conversion rate tends to increase with decreasing tube diameter due to a decreased dead volume.[70]

Flat tubular SOECs (Fig. 3iii) incorporate features from both planar and tubular designs. Here, multiple tubular gas channels made of cathode material are coated with solid electrolyte with the anode material being placed on top.

Switching from operating temperatures >600 °C to <80 °C, low-temperature electrolysers offer a broader range of products directly produced from CO_2 when compared to SOECs.[56,71] These electrolysers utilise liquid electrolytes while CO_2 is supplied at the backside of the gas diffusion electrode cathode. Typically, an ion exchange membrane is employed to separate the cathode and anode.[21]

In the zero-gap arrangement (Fig. 3iv) both electrodes are in direct contact with an ion-exchanging solid polymer electrolyte (SPE) membrane. While the anolyte flows on the backside of the anode, a humidified CO_2 stream provides the required water in the absence of a liquid catholyte.[72] Thus, by eliminating the gap between anode and cathode, this cell design not only offers the advantage of reduced ohmic resistance, but also simplifies scale-up by eliminating the need for separate electrolyte compartments.[73] The liquid fed (LF) zero gap cell (Fig. 3v) closely resembles the previous configuration, with the main difference being the supply of dissolved CO_2 as carbonate solutions *via* the liquid catholyte. This allows for the direct use of carbon capture solutions as a feed.[8,74]

By utilising distinct electrolyte compartments separated by a membrane, the dual flow arrangement (Fig. 3vi) enables a continuous flow of catholyte and anolyte at the respective electrode surfaces. The advantages of this cell design lie within the easily tuneable catalyst environment as well as the removal of liquid reaction products which can otherwise potentially lead to electrode and membrane degradation.[75] However, since the cathode surface is always in contact with a liquid, electrode flooding represents a major challenge for this reactor type.[76]

In the single flow (SF) catholyte configuration (Fig. 3vii), the catholyte flows between the cathode surface and the membrane,[77] while the anode is in direct contact with the membrane, receiving anolyte from the backside. In contrast, in the SF anolyte cell, the cathode is in direct contact with the membrane and is solely supplied with CO_2, while the anolyte flows between the membrane and the anode.[23]

A dual membrane configuration is typically used for the separation of liquid products or recovering CO_2 with help of a bipolar interface facilitating a cathodic gas diffusion electrode facing an anion exchange membrane and an anode facing a cation exchange membrane. The membranes are ionically connected with a porous solid electrolyte, which is purged with a humid gas or water to collect the liquid products or cross-over CO_2 (Fig. 3viii).

Instead of using membranes to separate the electrodes from each other, microfluidic cells (Fig. 3ix) achieve the separation of cathode and anode by utilising a laminar flow of electrolyte, while continuously transporting the reaction products along with this flow. This reactor design enables precise pH control and addresses water transport challenges commonly associated with membranes.[78]

4.2. CO_2-to-syngas/-carbon monoxide

Among the different possible CO_2 products, the conversion of CO_2 to CO as well as syngas (CO/H_2 mixture) represents not only one of the most investigated product routes (Fig. 2A), but also possesses the shortest transitional pathways for direct coupling with already established catalytic processes as determined through recent technoeconomic analyses.[79,80]

Notably, CO and syngas can be produced under electrolytic conditions using high-temperature solid-oxide electrolyser operating above 600 °C, as well as low-temperature electrolysers (25–80 °C). Within this section, we specifically focus on the generation of CO as the main target product rather than as an intermediate for multi-carbon (C_{2+}) products towards further C–C bonding. Those interested in further exploration of the subject are directed to additional literature reports and reviews that address the utilisation of carbon monoxide (CO) and carbon monoxide/carbon dioxide (CO/CO_2) mixtures in cascaded processes.[81–84]

4.3. High temperature electrolysis

CO_2-electrolysis at elevated temperatures using SOEC offers several advantages, including thermodynamic benefits, fast kinetics, and high conversion efficiency.[22,69,85] One of the key advantages lies within the possibility of using excess heat from other processes to decrease the cell potential, leading to overall improved energy efficiency. In evaluating the performance of CO_2 electrolysis using SOEC, it is important to note that the KPIs could not be applied to both high- and low-temperature electrolysis within the scope of our analysis. This difficulty arises due to a lack of explicit information, specifically in terms of faradaic efficiency for CO (FE_{CO}), on these parameters in the available literature. Specifically, in pure CO_2 electrolysis only CO is produced, resulting in nearly 100% FE_{CO} under normal operating conditions, often expecting full conversion.[22] However, when performing co-electrolysis of H_2O and CO, determining the FE_{CO} percentage is more difficult due to the simultaneous production of CO through the reverse water gas shift reaction (RWGS).[22] To consider the significant number of publications available, the comparison for SOEC is based on current density and cell voltage, rather than FE_{CO} or CO yield, as used in low temperature electrolysis. It is also worth noting that most publications focus on syngas production with varying H_2/CO ratios as the desired product.

Additionally, severe coking of the cathode is typically observed in pure CO_2 electrolysis as well in co-electrolysis of H_2O and CO_2, limiting the longevity of HT electrolysers. These

effects may be diminished by using reducing gases such as H_2, CH_4, or CO in the feed gas stream.[69] Specifically, pure CO_2 is used as the inlet gas in 94 out of 209 studies in our analysis. Since the composition of the input gas can also influence the cell potential, further emphasizing the challenge of comparing the performance of CO_2 electrolysis when using different inlet gas compositions.

The results of our literature analysis show that out of 210 publications, 50% demonstrate a current density between 410 and 6300 mA cm^{-2} (Fig. 4A), highlighting the potential for the industrial application of HT-reactors. Looking at the cell voltage for all cell types, the interquartile range (IQR) of the analysed publications (210) is spread from 1.3 V to 2.3 V (Fig. 4B).

Among the three cell types, the planar configuration is the most used and exhibits the highest current density values, with the median being 996 mA cm^{-2} and a 25th and 75th percentile of 521 mA cm^{-2} and 1605 mA cm^{-2}, respectively.

In comparison, the tubular configuration shows overall lower current density values compared to the planar cell, with a median of 410 mA cm^{-2}, a 25th percentile of 216 mA cm^{-2}, and a 25th percentile of 900 mA cm^{-2}. Efforts are being made to improve the conversion rates and consequently the current density of these electrolysers, by employing smaller tube sizes in micro tubular cells.[66,86] Additionally, tailoring the microstructure of tubular cells shows a significant impact on the performance, achieving the overall highest current density in our analysis, by using a micro-structured tubular SOEC with 6 channels integrated into the fuel electrode, the maximum current density reached 6260 mA cm^{-2} at a voltage of 1.8 V.[70]

The difference in current density between the two aforementioned SOEC types can be attributed to the longer current conduction pathways resulting in ohmic loss in the tubular cell design. In general, only a limited number of publications (9) is available for the tubular cell configuration possibly due to the higher level of manufacturing complexity involved.[87–93] The same limitation also applies to the flat tubular cell design and only 9 references could be considered for our comparison.[94–99] Moreover, the flat tubular configuration shows the narrowest distribution of current density with a 25th percentile of 300 mA cm^{-2} and a 75th percentile of 700 mA cm^{-2} and a median of 600 mA cm^{-2}.

Regarding the cell voltage values, upon closer examination, it can be observed that the median values for all three cell types have a difference of less than 0.2 V (Fig. 4B). The planar cell exhibits a voltage range, with minimum and maximum values of 0.6 V and 2.5 V, respectively, and a median voltage of 1.54 V. In line with the lower current densities mentioned earlier, the tubular cell type shows similar voltage values, with a median of 1.5 V. In comparison, the flat-tubular cell configuration demonstrates the widest distribution and highest median voltage of 1.8 V.

Focusing moreover on the observed long-term stability, planar reactors demonstrate a median operation time of 90 h (with an IQR of 30–120 h), whereas tubular reactors exhibit a median operation time of 100 h (with an IQR of 45–200 h), and

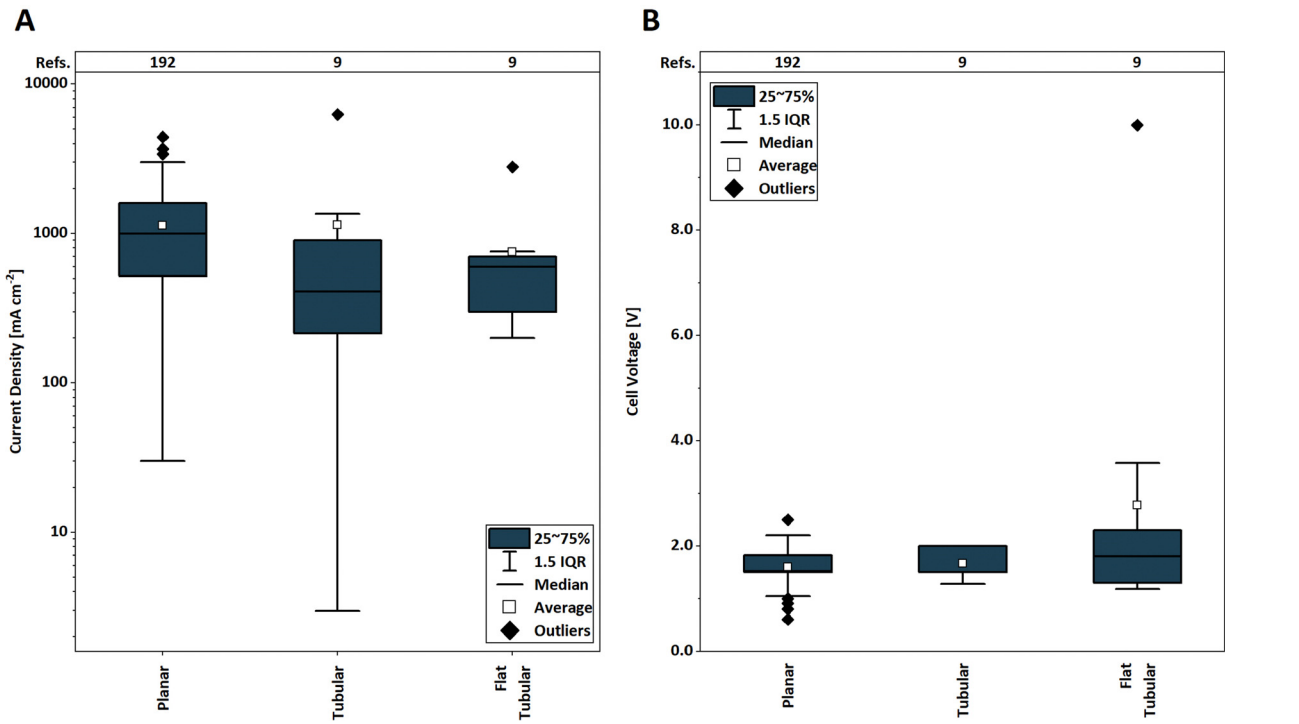

Fig. 4 Boxplots for the statistical evaluation of the current densities (left) and cell voltage (right) for the high-temperature electrochemical CO_2 reduction to CO achieved in the investigated reactor designs of 210 references.

flat tubular cells have a median operation time of 500 h (with an IQR of 400–900 h) (Fig. S7, ESI†). It should be noted that planar cells, despite having a lower median, exhibit the overall highest operation time of 3000 h in our comparison, while flat tubular cells also reached a high level of maturity by achieving an operation time of 1910 h.[99]

In terms of electrode size, the median electrode area of planar cells, most of which had small electrodes in the button format, is 0.5 cm^2 (with an IQR of 0.28–1 cm^2). Due to their geometric configuration, tubular and flat tubular cells, in general, exhibit larger active areas for the cathode or fuel electrode compared to planar cells. Tubular cells demonstrate a median electrode area of 3,14 cm^2 (with an IQR of 2.60–10.00 cm^2), while flat tubular cells exhibit a median electrode area of 60 cm^2.

Independently of the employed reactor design, the scalable production of tailored ceramic electrodes, possessing crucially addition to the necessary micro-structure, could possibly constitute one of the key limitations of novel designs such as tubular and flat tubular CO_2R, requiring further developments on both the material and electrode nano-structuring stage.[100,101]

4.4. Low temperature electrolysis

4.4.1. CO_2 – to – CO. Overall, zero-gap electrolysers as well as dual flow cells constitute the most employed reactor designs for the production of CO, followed by microfluidic configurations. Interestingly, the SF anolyte configuration, which utilises a liquid anolyte compartment, appears to be rarely employed (Fig. 5). In addition, recently, LF zero-gap cell types have emerged for CO/syngas generation, primarily through the conversion of liquid CO_2-capture solutions rather than direct conversion of gaseous CO_2.[74] Starting with the obtained FE values, in all cell configurations, the average faradaic efficiency for CO exceeds a value of 85%, highlighting the significant maturity of the field to selectively generate CO and syngas mixtures (Fig. 5B). One notable exception here constitutes LF zero-gap cell types demonstrating a mean value of 70% FE_{CO}. This slightly decreased value is attributed to the main use scenario of LF zero-gap cells, being the direct conversion of CO_2 capture solutions. In contrast to the direct conversion of gaseous CO_2, this process requires the balance of two competing processes: the selective regeneration of CO_2 within the electrolytic cell and its subsequent conversion in the capture solvent.[74,102–104]

Overall, cell configurations performing the direct conversion of gaseous CO_2 to CO, achieve median current densities $\geq$200 mA cm^{-2} at their highest FE_{CO} value, while the respective value for the LF zero-gap configuration currently lies close to 100 mA cm^{-2} (Fig. 5A). Though sparingly employed,[86–89] SF anolyte cells achieve the highest median and mean value with 290 and 334 mA cm^{-2} respectively, followed by zero-gap cells lying at 250 mA cm^{-2}. All in all, these values demonstrate that the low-temperature subfield of CO_2-to-CO conversion draws

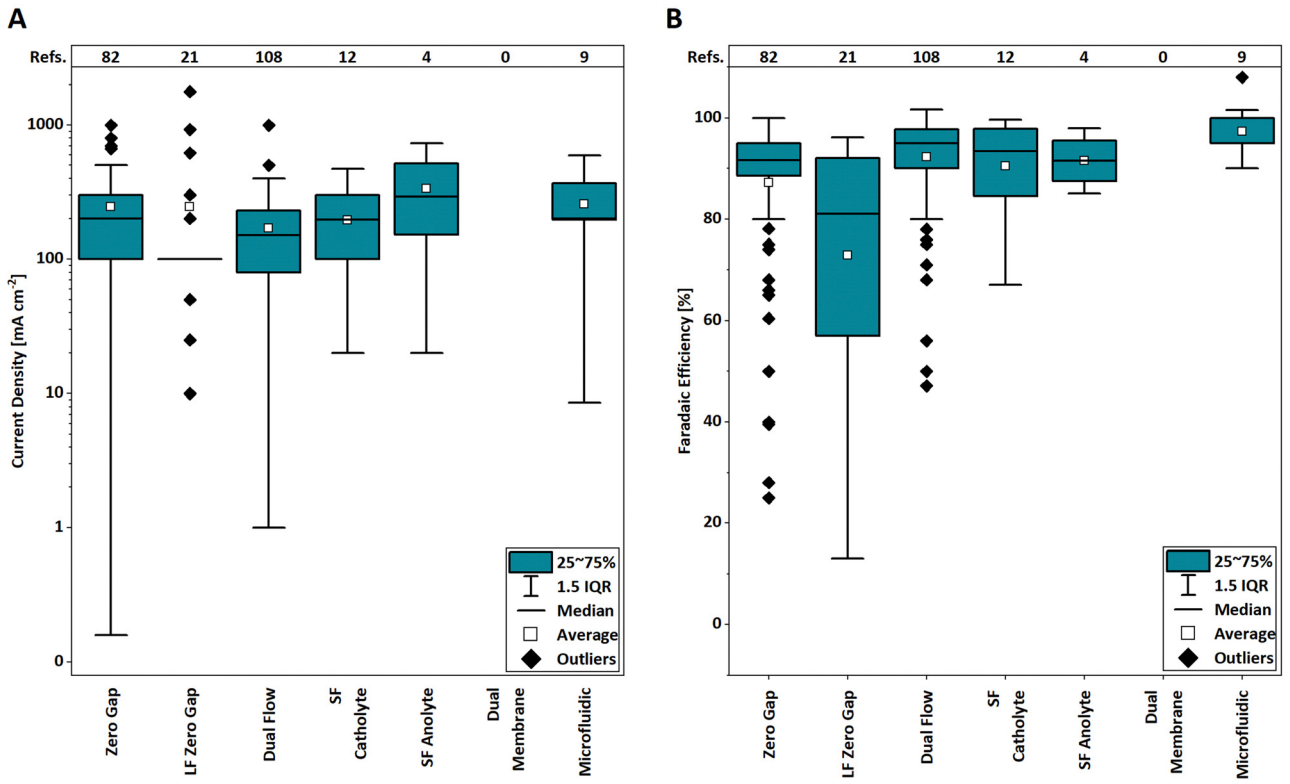

Fig. 5 Boxplots for the statistical evaluation of the current densities (left) and faradaic efficiencies (right) for the low-temperature electrochemical CO_2 reduction to CO achieved in the investigated reactor designs of 236 references.

steadily closer to the 200–500 mA cm^2 range that has been considered by multiple reports as one of the key metrics regarding industrial relevance.[90] Specifically, by employing high-carbonate conductance PiperION membranes, a j_{CO} value close to 1000 mA cm^{-2} employing a zero-gap cell operating at 60 °C has been reported,[53] whilst through the use of a CO_2 exsolution cell a j_{CO} value close to 1600 mA cm^{-2} was achieved in the case of LF zero-gap cell architecture, requiring though the frequent exchange of the employed cation-exchange membrane to maintain performance.[91]

Comparing the two most prevalent reactor architectures, zero-gap and dual flow, the former has recently established itself as the more industrially relevant option, due to its comparatively higher energy efficiency and demonstrated ability to operate under dynamic conditions, employing similar materials and production process to the PEM and AEM based water electrolysers.[105–107] It is though important to mention that within our analysis we have also observed an increasing emergence of investigations based on LF zero gap architectures, exploring their advantage to be coupled directly to CO_2 capture installations.[8,108] Notably, as already highlighted before, the large-scale establishment for the electrolytic conversion of CO_2 can only be achieved by ensuring elevated selectivity at longer timescales. Overall, both zero gap and dual flow cells have shown the ability to perform CO_2 electrolysis for 100 h at applied current densities >100 mA cm^{-2}, with the longest reported zero gap report showing operational stability being 3800 h at 200 mA cm^{-2} (FE_{CO} >90%), while in the case of dual-flow electrolysers they have been shown to maintain a FE_{CO} value of 90% at 300 mA cm^{-2} for 1500 h.[109,110] (Fig. S8A, ESI†). Evidently, breaking through the 100-h testing barrier may also constitute a difficult endeavour to achieve in lab-scale environments, prompting the need for dedicated tested set-ups as well as of improved testing protocols under tailored conditions, in which promising electrodes/reactors are directly tested at $j \geq$ 300 mA cm^{-2} to decreasing testing time.[111,112]

This automated long-term testing must also be performed under industrially relevant active areas, with the majority of cell areas for LT-CO generation lying close to or below 10 cm^2 (Fig. S8, ESI†). Furthermore, operational temperature and pressure play an equally important role in the industrial relevance of an investigation as the achieved KPIs. It is therefore necessary to transition LT-CO_2R investigations beyond ambient conditions and closer to application-oriented conditions (temperature: 60–80 °C, pressure 1–10 bar).[113]

4.2. CO_2-to-formate/-formic acid

According to the findings of this study, the reduction of CO_2 to formic acid or formate has been identified as the second most prevalent research area within the domain of low-temperature CO_2 electrolysis (Fig. S1, ESI†). In general, dual flow reactors are the two most employed reactor types, making up ~70% of the analysed literature followed by zero gap.

The faradaic efficiency of all the reactor types exhibits a median FE_{HCOOH} of >80%, thereby demonstrating the maturity of the field in this case (Fig. 6B). With regard to current density, all reactor types have the capacity to attain a maximum of at least ~10 mA cm^{-2}, with median values exceeding 100 mA cm^{-2}. Here, SF catholyte reactors present the highest median values. Nonetheless, given the substantial quantity of references, dual-flow reactors also exhibit considerable current densities, with median and average values exceeding 200 mA cm^{-2}. In addition, the median value of SF anolyte reactors is 90 mA cm^{-2}. Conversely, zero gap reactors have demonstrated the lowest median value to date. A comprehensive evaluation of the median values for the FE_{HCOOH} and current density reveals that dual flow and SF catholyte reactors emerge as the most promising designs for the reduction of CO_2 to formic acid/formate. The underlying reason for this phenomenon is their capacity to exert precise control over the pH level within the catalytic layer. This ability is accompanied by the utilisation of cation exchange membranes, which serve to reduce the occurrence of formate crossover.[25]

The highest current density recorded for any reactor design, including outliers, was achieved in a dual flow cell configuration. This configuration yielded a value of 1800 mA cm^{-2} and a FE_{HCOOH} of 74% over a period of 45 min. The experiment utilised a 1 cm^2 cathode with tin oxide as the catalyst.[114]

In the context of SF catholyte reactors, it has been determined that a current density of 1200 mA cm^{-2}, in conjunction with a FE_{HCOOH} of 100%, yields a substantial current density.[115] Furthermore, a current density of 677 mA cm^{-2} with a FE_{HCOOH} of 83% was also achieved.[116]

In the context of zero gap reactors, the second most researched reactor type, the highest reported current density is approximately 800 mA cm^{-2} at 3.4 V.[117] Furthermore, in our analysis is 400 mA cm^{-2} with a FE_{HCOOH} of 85%.[118] This was achieved by developing In/In_2O_3 hollow nanotubes, which enhance the CO_2R activity at the active In^0 sites, while the oxidised In^{3+} species mitigates the hydrogen evolution reaction (HER). It is important to note that, in order to achieve long-term performance, the anolyte containing formate had to be replaced ''every few hours'' due to the zero gap cell configuration with an anion exchange membrane (AEM). This replacement was necessary to prevent anolyte acidification and oxidative decomposition of formate.[118]

In order to perform a more comprehensive evaluation of the industrial maturity of the CO_2 electrolysis process for formic acid production, it is necessary to consider the operational time. As illustrated in Fig. S9 (ESI†), certain reactor types have been observed to operate for a duration of at least 100 h. In this instance, dual membrane reactors exhibited the highest median value, reaching approximately 100 h, with a high value of 1000 h. This was achieved on a 3 cm^2 cell at a cell voltage of 3.6 V and at elevated current densities (≥200 mA cm^{-2}).[105]

With regard to the duration of electrolysis, the performance of the other reactors was nearly equivalent. However, dual flow reactor designs showed promising individual potentials. 400 h of electrolysis are achieved by using a 1 cm^2 cell with a current density of 250 mA cm^{-2}.[106] Analysed by synthesizing an indium nanosheet, a stable long-term operation of 140 h was reported in an SF catholyte reactor.[107] Using a 16 cm^2 electrode, a

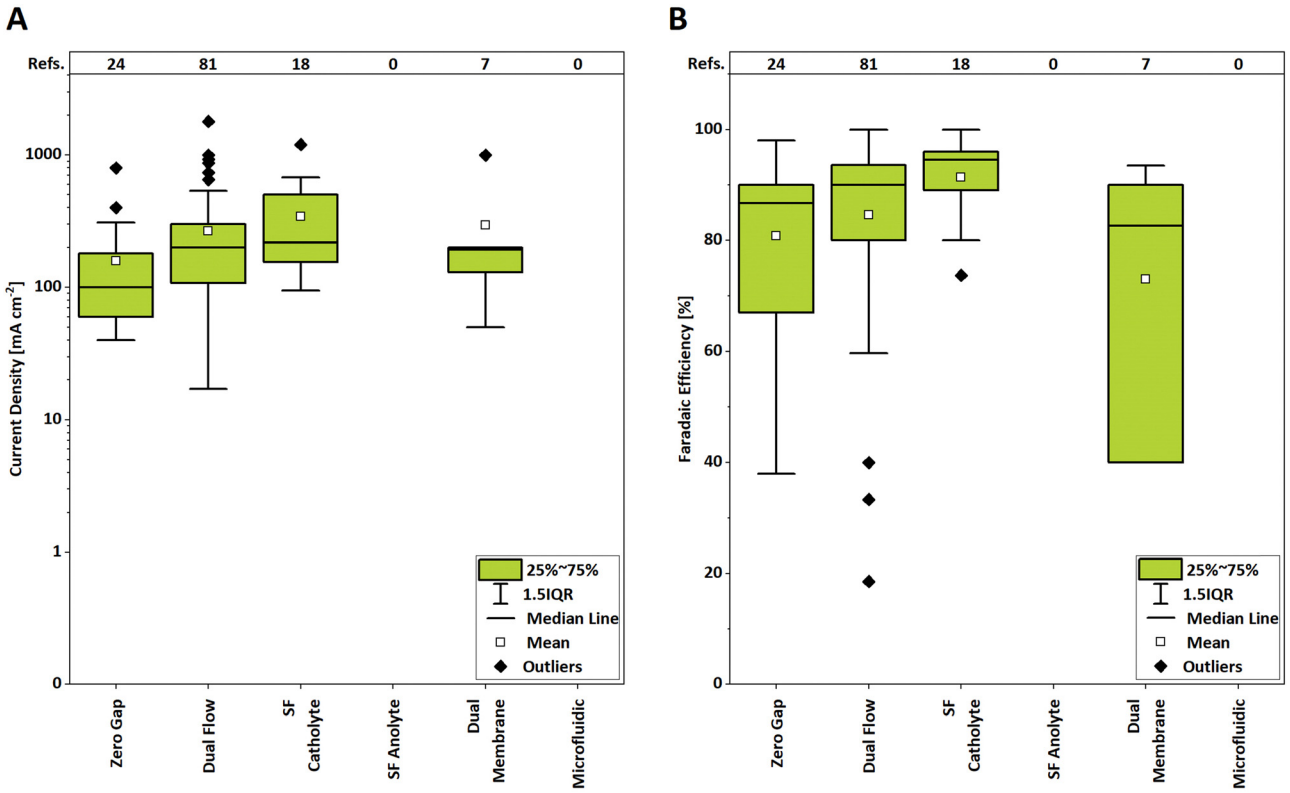

Fig. 6 Boxplots for the statistical evaluation of the current densities (left) and faradaic efficiencies (right) for the electrochemical CO_2 reduction to formic acid/formate achieved in the investigated reactor designs of 130 references. In the case of liquid products such as formate and formic acid, the zero gap cell was not differentiated between the zero gap and the LF variant.

FE_{HCOOH} >90% with a cathode potential of −1.04 V *vs.* RHE at 100 mA cm $^{-2}$ was maintained throughout the experiment. For a zero gap reactor, the highest reported operation time is 200 h at 100 mA cm^{-2}.[108]

Thus, although dual flow reactors represent the state-of-the-art reactor design for the reduction of CO_2 to formic acid/formate, there are promising alternatives such as SF catholyte and dual membrane reactors that can show similar or improved performances for certain KPIs. The dual membrane outperformed the dual flow reactor in terms of electrolysis duration on individual scale by a large number regardless of being less studied. This shows that the dual membrane has the highest potential to be studied on a larger scale on an industrial level due to its ability to produce pure formic acid by using deionised water.

4.3. CO_2-to-C_2 (ethylene and ethanol)

According to our literature scope, ethylene represents the CO_2R product with the highest market demand due to its use as a precursor for several synthetic bulk products (*i.e.* ethylene oxide, styrene, polyethylene, polyesters).[119–121] At the same time, recent advances in CO_2R technologies have showcased the ability of new Cu-based materials to generate multi-carbon hydrocarbons and oxygenates beyond ethylene and methane, such as alcohols and acids, which could potentially be interesting in niche-market applications.[122] Specifically, ethylene and ethanol constitute, according to our analysis, the two most prominent products during CO_2R on Cu-based electrodes in current literature, with the achieved KPIs for 1-propanol or acetic acid yet lying far behind. Since from the viewpoint of reaction mechanics ethylene and ethanol are competing products, the important challenge in recent years has become to effectively control the competition between the two C_{2+} products, as ethylene tends to be the default one.[123] Thus our following discussion will thus initially focus on the effect of controlling the ethylene: ethanol selectivity, expressed in terms of the achieved FE values, prior to discussing the current state-of-the-field on production of these two competing products on the different reactor types (Fig. 7 and Fig. S10, ESI†). Here, our complete box-plot analysis for all different C_{2+} products can be found in the ESI.† Notably, production of ethylene as the unique C_{2+} product seems to be well controlled, with interesting current densities between 125 and 292 mA cm^{-2} in dual flow, around 164 mA cm^{-2} in zero gap and close to 122 mA cm^{-2} in microfluidic reactors. This marginal selectivity towards ethylene seems not to be the case towards ethanol. Indeed until 2023, reports on the complete suppression of ethylene in favour of the alcohol had only succeeded at very low current densities <20 mA cm^{-2}, albeit at elevated FE values of >70% in such cases.[124–126] Thanks to progress in catalyst engineering, selectivity towards multi-carbon alcohols has been significantly improved. Regardless of the value of applied current, numerous

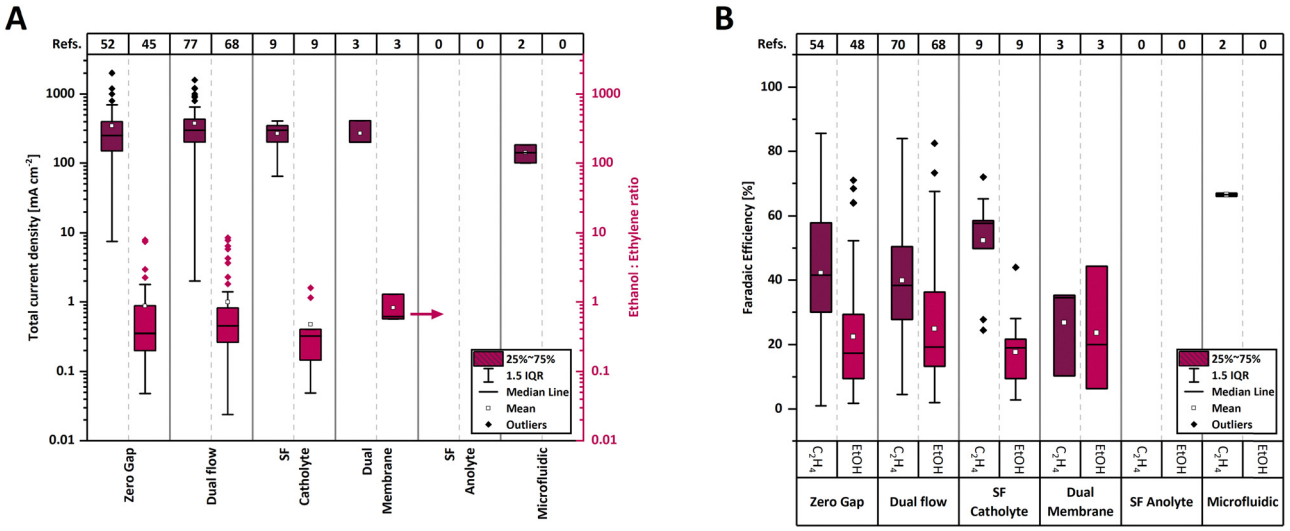

Fig. 7 Boxplots for the statistical evaluation of the total current densities achieved for ethanol and ethylene alongside the FE_{EtOH}:FE_{C2H4} ratio (left) and faradaic efficiencies (right) for the generation of ethylene and ethanol in the investigated reactor designs of 268 references.

studies have reported on ethanol production with $FE_{Ethanol}$/$FE_{Ethylene}$ ratios over 1.5 for dual flow, single-flow catholyte and zero-gap reactors (Fig. 7-A). Investigations were performed in dual flow and zero gap cells reaching in some cases ethanol: ethylene ratios above 5, while complete ethylene suppression being also achieved producing ethanol with a FE value of 67% faradaic efficiency at an industrially relevant current density of 186.5 mA cm^{-2} in a dual flow reactor.[127]

Focusing on the selective production of ethylene, our analysis shows that electrochemical reactor designs for the direct conversion of CO_2 to ethylene mostly consist of membrane reactors. Here, zero gap and dual flow electrolysers represent the state-of-the-art reactor designs, with 49 and 70 KPI-fulfilling reports respectively, followed by SF catholyte, dual membrane and microfluidic reactors. Primarily, ethylene is produced at current densities of more than 500 mA cm^{-2}, mainly using dual flow, single flow catholyte and zero gap reactors. Secondarily, the production of alcohols, essentially ethanol and to a lesser extent propanol, is currently achieved with an elevated current density between 300 and 500 mA cm^{-2} in dual flow and zero gap cells. With membrane-based reactors, ethylene production shows almost the same median current densities at around 200 mA cm^{-2}. The same pattern is observed with ethanol, but at a lower median value around 100 mA cm^{-2}. However, the scarcity of references for dual membrane and microfluidic reactors limits statistical significance of these boxplots, meaning that zero gap and dual flow reactors present the most mature technologies in this field. In terms of total current density for the selective production of ethanol and ethylene, all reactor types show the capability to operate above 200 mA cm^{-2}, with median values close to 400 mA cm^{-2} for dual flow, SF catholyte and zero gap technologies, which are the most investigated ones. Total current densities above 1 A cm^{-2} have been achieved for zero gap and single flow catholyte reactors while in the case of dual flow reactors an impressive value of 1.6 A cm^{-2} was achieved. Yet, the 40-h stability was only proven at 400 mA cm^{-2}.[128] It is worth pointing out that in the high current density range (typically >800 mA cm^{-2}), not only are interesting selectivity towards C_{2+} products observed with dual flow and zero gap reactors but also the promotion of alcohols (indicated by the ethanol to ethylene ratios >1) for both technologies. Three publications have been reported on the use of the dual membrane technology for the electroconversion of CO_2 with copper-based catalysts at total current densities between 200 and 410 mA cm^{-2} and the particularity of generating ethanol at relatively high purity levels between 13.1 wt% and 90% through the solid-state electrolyte.[129–131] But the selectivity of the target products on this technology remains low with 42 and 71 mA cm^{-2} for ethylene and between 26 and 89 mA cm^{-2} for ethanol.

5. Discussion

5.1. Categorization of CO_2 sources - sinks & coupling scenarios

Achieving a closed carbon cycle on an industrial scale necessitates the customisation of the characteristics of the various CO_2 point sources and CO_2R electrolysis technologies within a multitude of multifaceted scenarios. Within this study, we have decided to structure the following discussion transitioning from the characteristics of CO_2 point sources to the different scenarios. It is conceivable that such a scenario could be realised within the confines of a closed-carbon economy, complemented by technologies that demonstrate optimal compatibility with these circumstances.

The findings of the present study demonstrate that cement plants, followed by waste incineration and pulp plants, are and will continue to be the three primary sources of CO_2 emissions in Europe (and potentially around the globe). It is crucial to note that these sources are able to meet the demand for carbon-

based chemicals through their emissions until 2050. Common characteristics of the mentioned sources is that they emit CO_2 in the Mt-scale annually, being able to directly provide heat to coupled electrolytic systems, operating overall in a highly centralised manner. While not considered within our report, the production of steel could also be another possible point source that shares these characteristics. Currently, the selected route towards its defossilisation being either an integration to CCU processes, or the establishment of green steel, appears to be influenced primarily by policy makers. Hence, a more in-depth analysis over the associated advantages and disadvantages of each route, in a case-by-case scenario, is required in this case.[33,35]

In contrast, potential sink products and sites, such as chemical producers, necessitate substantial amounts of CO_2R products, including CO, syngas, and ethylene. However, these entities predominantly lack the capacity to fully satisfy their carbon requirements through on-site CO_2 emissions. Furthermore, we anticipate that direct air capture will become increasingly influential in supplying this closed carbon cycle in the forthcoming years, as emissions from other industries are reduced through advancements in energy efficiency.

In sum, by integrating the various components of the source-electrolyser-sink system, the three following distinct scenarios for the establishment of a CO_2-based circular economy emerge:

I. A source-centralised scenario, in which CO_2 reduction and chemical manufacturing take place at point source site.

II. A sink-centralised scenario, in which CO_2 is provided to a chemical manufacturing site *via* multiple pathways.

III. A fully decentralised scenario, which is based on the performing CO_2 electrolysis in remote locations at which renewable electricity is readily available and highly cost-efficient (Fig. 8).

In the source-centralised scenario (Fig. 8) a major point source, such as cement plant, would either provide capture CO_2 to industrial sink-sources or perform CO_2 electrolysis on-site towards direct value chain of the associated CO_2 emissions. In this case, waste-incineration plants present a highly intriguing prospect, given their capacity to provide the requisite CO_2 emissions, electricity, and heat necessary to facilitate this process. Furthermore, in this source-centralised scenario, an additional open question is the associated cost of on-site chemical manufacturing, especially in the case of only one industrial stakeholder, necessitating substantial investments to fully leverage the advantages of such a centralised solution.

Here, another pragmatic alternative to consider is the implementation of a CO_2 pipeline. In this scenario, emissions from processes with high CO_2 intensity would be transported to electrified chemical hubs for additional value chains. This approach would establish a sink-centralised scenario, lies more on the side of on managing and reducing CO_2 emissions.

It is imperative to acknowledge that the vast majority of chemical manufacturers are incapable of directly supplying the requisite amount of CO_2 emissions necessary to execute CO_2R on a large scale. Nevertheless, there is an ongoing demand for CO_2R-derived products, whether as direct chemicals in their processes or as significant building blocks, such as syngas or ethylene.

In contrast, the sink-centralised counterpart scenario (Fig. 8) requires tailoring on both the CO_2 emissions and the target CO_2R-product sides. An example of a sink-centralised source includes here the production of small-volume chemicals, such as diisocyanates, which are utilised in glues, powder coatings, and foamed rubber *via* carbonylation reactions (or *via* phosgene). Specifically, in Europe the largest plant for the production of toluene diisocyanate (TDI) with a capacity of 300 000 tons per year is currently operated by Covestro in Germany.[132]

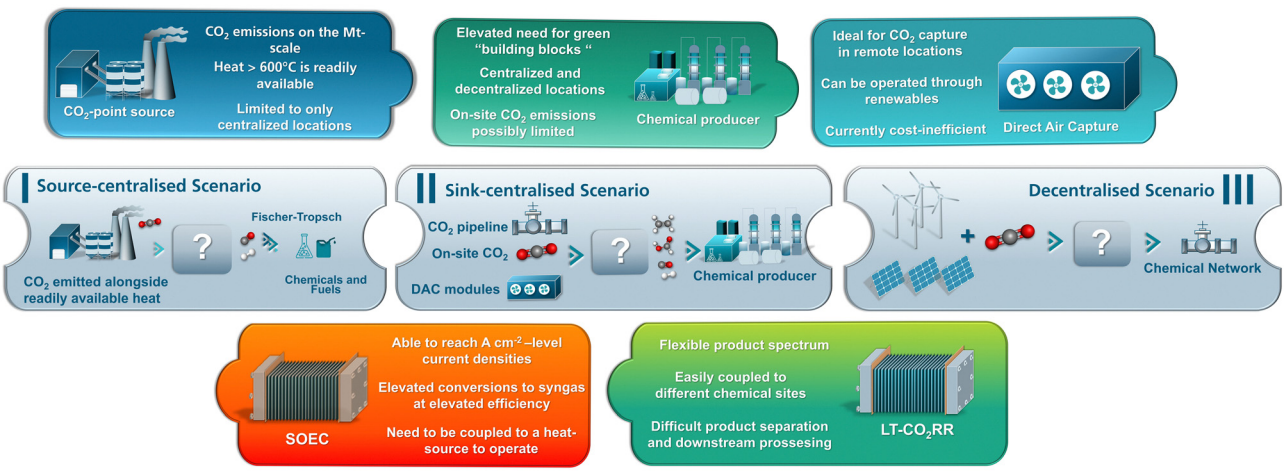

Fig. 8 Schematic representation of the "puzzle-pieces" between source (top row) and sink (bottom row) matching in the different scenarios. The pieces are deliberately not connected since technologies be individually tailored for each envisioned scenario. Therefore, the middle row can only envisage as exemplary scenarios which are not fully fixed in their composition. A typical value chain (complete puzzle) is consisting of all three parts (top, middle, bottom).

This is equivalent to approximately the use of 100 000 tons of CO per year. To achieve this, MW-scale implementations of CO_2-to-CO electrolysers are necessary, while concurrently reducing the CO_2 footprint by 160 000 tons per year. This would result in a 17% reduction in the global warming potential of TDI alone.[133] Furthermore, this example illustrates the potential for establishing centralised locations that function as electrified hubs. In these hubs, CO_2 is transformed into primary building blocks prior to being transported and subsequently processed in neighbouring plants *via* short pipelines. In such a case, CO_2 could be provided by a multitude of sources, ranging from the aforementioned CO_2 pipeline, on-site emissions, or DAC modules.

Furthermore, in the case of the third fully decentralised scenario, which is based on remote locations, its implementation is contingent on the specific location and the type of product generated. Evidently, optimal locations for the establishment of this scenario would be those with inexpensive and abundant renewable electricity. Here, Southern Mediterranean Europe and Scandinavian countries seems to be the most promising regions within the European Union. In addition, integration of biodigesters and wastewater treatment could provide a decentralised CO_2 source, supporting chemical electrification and carbon cycle closure. In this case, further studies are needed to assess their use in electrolysis beyond microbial electrolysis for methane production.[36,37,134] Most crucially though, in this decentralised scenario, the potential target CO_2R products are contingent upon the customer's utilisation.

From our analysis, formic acid could hold the potential to satisfy the demands of this remote-based scenario. The utilisation of formic acid or its salts extends to various applications, including de-icing agents, fertilizers, drilling fluids, and heat transfer fluids.[135] However, it should be noted that the cost associated with formic acid can be particularly significant, particularly when it is sold at a premium price in the context of sustainability. Prospectively, a shift to the utilisation of formic acid as a liquid carrier for carbon monoxide (CO) or hydrogen (H_2) may present further viable business opportunities, particularly in the context of the increasing prevalence of centralised scenarios in large-scale applications.[136] On the other hand, the on-site production of green bulk chemicals in Central Europe is not a viable option due to the inherent limitations of the renewable energy supply. These topological limitations indicate that, at the European level, a more robust collaboration between member states is necessary. Such collaboration should focus on the production of renewable electricity in excess amounts, as well as on the establishment of hubs for capture, storage and transport CO_2 emissions coupled to subsequent chemical manufacturing. Moreover, in order to establish a fully decentralised scenario in the coming decades, as DAC becomes even more prevalent, it will also be necessary to rethink our CO_2 value chain pathways. From a technological perspective, Table S2 (ESI†) and Fig. 8 provide a synopsis of the salient features and merits of the various HT and LT technologies of CO_2R, as outlined in our preceding technical review. Specifically, state-of-the-art SOEC electrolysers have demonstrated the capacity to attain current densities of up to 1000 mA cm^{-2}, accompanied by elevated CO_2 conversion values, allowing for the production of tailored syngas compositions. Nevertheless, the efficient operation of SOECs requires direct coupling to sites, where heat at elevated temperature is readily available. This strong dependency of efficiently operated SOEC to large-scale heat sources, such as cement plants, makes them more suitable for centralised scaled-up applications to fully take advantage of this technology. Notably, since SOECs frequently exhibit elevated CO_2 conversion capabilities, they also facilitate their direct integration with FT reactors towards the on-site generation of multi-carbon products. Conversely, low-temperature CO_2R technologies exhibit enhanced flexibility in their application and can be utilised in both centralised and decentralised manners. As already shown, these technologies have the capacity to generate a range of CO_2R products, operating within temperature conditions (60–80 °C) that can be readily accommodated by large-scale chemical production facilities. Moreover, on the integration side, research has also demonstrated that LT-CO_2R systems possess the capacity to be integrated with FT-reactors and exhibit a rapid adaptability to the voltage spectrum of PV modules, particularly in the context of decentralised systems.[137] Nevertheless, regarding the latter the actual flexibility of a deployed LT-CO_2R electrolyser is dependent on the complete system design, including downstream processing and purification. As demonstrated in our analysis of LT-CO_2R, the conversion of CO_2-to-CO is the most mature conversion pathway, followed by the conversion to formic acid and ethylene. Moreover, while the production of alcohols directly from CO_2 could be highly interesting for the chemical industry, their direct production currently still suffers from issues of selectivity and long-term stability and elevated current densities. Nevertheless, in the case of LT-CO_2R, there exists a crucial necessity the necessity for acceleration in two key areas: the achieved conversion and the overall energy efficiency of LT-CO_2R electrolysers. Only through in these key metrics can the low-temperature technological route effectively compete within the industrial scale, with the more straightforward hight-temperature one.[105]

While our discussion offers some possible improvement strategies regarding the transition of CO_2 electrolysis to a truly industrially and environmentally impactful technology, its viability can only be truly assessed at the system level, with integration into the existing infrastructure remaining another crucial issue to be addressed. Questions to address here include the access to renewable energy, tolerance to trace impurities in CO_2 feedstocks, and compatibility with downstream processing are critical factors influencing feasibility at scale. Notably, most studies still rely on high-purity CO_2 feeds, overlooking the complexity of real gas streams from capture systems, which may impact catalyst stability and product purity. Moreover, both source-centralised and sink-centralised configurations necessitate tailored adaptation of CO_2R technologies to align with existing industrial and energy networks. The transition to large-scale deployment is further constrained by the dependence on noble-metal anodes, particularly IrOx,

which are also essential for PEM electrolysers, creating competition for scarce resources. Addressing these challenges requires iterative refinement of reactor designs, process configurations, and materials to ensure compatibility across different industrial scenarios. Thus, while CO_2R holds promise as a key enabling technology for a closed-carbon economy, its realization and viability depends on coordinated efforts across catalyst development, electrolyser engineering, and system-level integration strategies within datasets beyond the lab-scale integration drawing closer to the kW and MW scale of integration.[105]

In summary, the establishment of a closed-carbon economy cannot be regarded as a unidirectional undertaking. The intricate interplay among point sources, sinks, and electrolysis products, both in centralised and decentralised configurations, weaves a multifaceted tapestry. This complexity necessitates further customization of each HT and LT technology to its respective scenario. As a result, while recommendations can be made concerning the most suitable CO_2R reactors for various scenarios, these recommendations must undergo numerous iterations of refinement, both in terms of schematics and on-site adaptations, to ensure optimal functionality and compatibility.

6. Conclusions

In conclusion, through our extensive techno-economic and literature research, our article provides both researchers and industrial stakeholders with a clearer roadmap on the when, where, how and for which product, CO_2 electrolysis can be an attractive technology. This investigation reveals the necessity of a stone-laying framework that prioritises low-volume, high-price scenarios prior to the expansion of the technology to commodity chemicals. This necessity is underscored by an analysis of current and projected CO_2 emissions and market demands up to the year 2050. Similarly, we envision that the type of CO_2-source operating large-scale CO_2 electrolysis technologies will transition through three stages, from: (a) directly CO_2-industrial point-sources, through (b) a mixture of CO_2 point-sourcing and DAC, to (c) the primary establishment of DAC as the CO_2 provider, alongside unavoidable large-scale emitters, such as cement and waste incineration plants.

At the same time, we present three scenarios on how such an electrochemical CO_2R-based chemical economy could look like, highlighting the need to further explore the role of point sources to act as electrified hubs for providing CO_2 through dedicated pipelines as well as creating centralised solutions to produce chemicals.

Finally, it is imperative to underscore the necessity to enhance the optimization and standardization of data reporting and dissemination within the scientific electrochemical community. Through this holistic examination, our work contributes to advancing the discourse on the prospects of CO_2 electroreduction, accelerating innovation and targeted decision-making in the CO_2 electrolysis field.

Author contributions

Data curation, methodology, investigation, writing – original draft: Muhammad Tayyab, Maximiliane Dreis, Dennis Blaudszun, Kevinjeorjios Pellumbi, Urbain Nzotcha, Muhammad Qaiser, Kai junge Puring, and Hermann Tempel; writing – revision: Muhammad Tayyab, Maximiliane Dreis, Dennis Blaudszun, Kevinjeorjios Pellumbi, Urbain Nzotcha, Kai junge Puring, Hermann Tempel and Rüdiger-A. Eichel; conceptualization, supervision, funding acquisition: Sebastian Stießel, Kai junge Puring, Ulf-Peter Apfel, Henning Weinrich, Hermann Tempel and Rüdiger-A. Eichel.

Data availability

All data used within the box-plot analysis as well as source-sink matching are available in tables in the ESI.†

Conflicts of interest

There are no conflicts to declare.

Acknowledgements

The authors thank the Ministry for Economy, Innovation and Digitalization and Energy (MWIDE) of the state of North-Rhine Westphalia for funding within the SCI4Climate Cluster, Project ElektiCO_2NRW-Nr. EFO/0086A and EFO/0086B. Ulf-Peter Apfel. was funded by the Deutsche Forschungsgemeinschaft (DFG, German Research Foundation) under Germany's Excellence Strategy - EXC 2033-390677874–RESOLV as well as APAP242/9-1, the Fraunhofer Internal Programs under grant no. Attract 097-602175 and ''MAT4HY-NRW'' (KP22-065-A) grant for the state NRW. The authors from FZJ kindly acknowledge funding by the Federal Ministry of Education and Research (BMBF), Project: iNEW2.0 ''Inkubator Nachhaltige Elektrochemische Wertschöpfungsketten'' Funding code: 03SF0627A. The authors gratefully acknowledge Mr. Sebastian Lehmann for his contribution in creating the table of contents figure for this article.

References

1 C. Sapart, A. Perimenis and T. Bernier, *The Contribution of Carbon Capture & Utilisation towards Climate Neutrality in Europe*.
2 *European Commission, Net-Zero Industry Act*, **https://commission.europa.eu/strategy-and-policy/priorities-2019-2024/european-green-deal/green-deal-industrial-plan/net-zero-industry-act_en**, (accessed 7 July 2024).
3 G. Centi and S. Perathoner, The chemical engineering aspects of CO_2 capture, combined with its utilisation, *Curr. Opin. Chem. Eng.*, 2023, **39**, 100879.
4 F. Nath, M. N. Mahmood and N. Yousuf, Recent advances in CCUS: A critical review on technologies, regulatory aspects and economics, *Geoenergy Sci. Eng.*, 2024, **238**, 212726.

5 S. Tasleem, C. S. Bongu, M. R. Krishnan and E. H. Alsharaeh, Navigating the hydrogen prospect: A comprehensive review of sustainable source-based production technologies, transport solutions, advanced storage mechanisms, and CCUS integration, *J. Energy Chem.*, 2024, **97**, 166–215.
6 R. Sen and S. Mukherjee, Recent advances in microalgal carbon capture and utilization (bio-CCU) process vis-à-vis conventional carbon capture and storage (CCS) technologies, *Crit. Rev. Environ. Sci. Technol.*, 2024, 1–26.
7 P. de Luna, C. Hahn, D. Higgins, S. A. Jaffer, T. F. Jaramillo and E. H. Sargent, What would it take for renewably powered electrosynthesis to displace petrochemical processes?, *Science*, 2019, **364**, eaav3506.
8 D. J. D. Pimlott, Y. Kim and C. P. Berlinguette, Reactive Carbon Capture Enables CO_2 Electrolysis with Liquid Feedstocks, *Acc. Chem. Res.*, 2024, **57**, 1007–1018.
9 W. A. Smith, T. Burdyny, D. A. Vermaas and H. Geerlings, Pathways to Industrial-Scale Fuel Out of Thin Air from CO_2 Electrolysis, *Joule*, 2019, **3**, 1822–1834.
10 O. J. Guerra, H. M. Almajed, W. A. Smith, A. Somoza-Tornos and B.-M. S. Hodge, Barriers and opportunities for the deployment of CO_2 electrolysis in net-zero emissions energy systems, *Joule*, 2023, **7**, 1111–1133.
11 *Novo Nordisk Fonden, CO_2 as a sustainable raw material in our future food production - Novo Nordisk Fonden,* **https://novonordiskfonden.dk/en/news/CO2-as-a-sustainable-raw-material-in-our-future-food-production/**, *(accessed 7 July 2024).*
12 O. S. Bushuyev, P. de Luna, C. T. Dinh, L. Tao, G. Saur, J. van de Lagemaat, S. O. Kelley and E. H. Sargent, What Should We Make with CO_2 and How Can We Make It?, *Joule*, 2018, **2**, 825–832.
13 S. van Bavel, S. Verma, E. Negro and M. Bracht, Integrating CO_2 Electrolysis into the Gas-to-Liquids–Power-to-Liquids Process, *ACS Energy Lett.*, 2020, **5**, 2597–2601.
14 R. Daiyan, I. MacGill and R. Amal, Opportunities and Challenges for Renewable Power-to-X, *ACS Energy Lett.*, 2020, **5**, 3843–3847.
15 S. R. Foit, I. C. Vinke, L. G. J. de Haart and R.-A. Eichel, Power-to-Syngas: An Enabling Technology for the Transition of the Energy System?, *Angew. Chem., Int. Ed.*, 2017, **56**, 5402–5411.
16 C. Wulf, P. Zapp and A. Schreiber, Review of Power-to-X Demonstration Projects in Europe, *Front. Energy Res.*, 2020, **8**(191), 1–12.
17 *BCG Global, Boston Consulting Group Builds Partnership with Twelve to Support Innovation in Sustainable Aviation Fuel*, **https://www.bcg.com/news/15may2024-bcg-partnership-innovation-in-sustainable-aviation-fuel**, (accessed 7 July 2024).
18 *Breakthrough Energy, Dioxycle's Groundbreaking Electrolyzer Transforms Carbon Emissions into Valuable Assets | Breakthrough Energy*, **https://www.breakthroughenergy.org/news/dioxycle-groundbreaking-electrolyzer/**, (accessed 7 July 2024).
19 *Breakthrough Energy*, CERT Systems Inc, **https://www.breakthroughenergy.org/fellows-project/cert-systems-inc/**, (accessed 7 July 2024).
20 *FlowPhotoChem, Industry interview and overview: a closer look at eChemicles*, (accessed 7 July 2024).
21 D. Wakerley, S. Lamaison, J. Wicks, A. Clemens, J. Feaster, D. Corral, S. A. Jaffer, A. Sarkar, M. Fontecave, E. B. Duoss, S. Baker, E. H. Sargent, T. F. Jaramillo and C. Hahn, Gas diffusion electrodes, reactor designs and key metrics of low-temperature CO_2 electrolysers, *Nat. Energy*, 2022, **7**, 130–143.
22 Y. Song, X. Zhang, K. Xie, G. Wang and X. Bao, High-Temperature CO_2 Electrolysis in Solid Oxide Electrolysis Cells: Developments, Challenges, and Prospects, *Adv. Mater.*, 2019, **31**, e1902033.
23 Á. Vass, A. Kormányos, Z. Kószó, B. Endrődi and C. Janáky, Anode Catalysts in CO_2 Electrolysis: Challenges and Untapped Opportunities, *ACS Catal.*, 2022, **12**, 1037–1051.
24 H. Shin, K. U. Hansen and F. Jiao, Techno-economic assessment of low-temperature carbon dioxide electrolysis, *Nat. Sustainability*, 2021, **4**, 911–919.
25 D. Ewis, M. Arsalan, M. Khaled, D. Pant, M. M. Ba-Abbad, A. Amhamed and M. H. El-Naas, Electrochemical reduction of CO_2 into formate/formic acid: A review of cell design and operation, *Sep. Purif. Technol.*, 2023, **316**, 123811.
26 K. Fernández-Caso, G. Díaz-Sainz, M. Alvarez-Guerra and A. Irabien, Electroreduction of CO_2: Advances in the Continuous Production of Formic Acid and Formate, *ACS Energy Lett.*, 2023, **8**, 1992–2024.
27 *European Commission, 06.02.2024, Strasbourg, Communication from the commission to the European Parliament, the council, the European Economic and Social Committee and the Committee of the Regions - Towards an ambitious Industrial Carbon Management for the EU, EUR-Lex - 52024DC0062 - EN - EUR-Lex*, **https://eur-lex.europa.eu/legal-content/EN/TXT/?uri=COM%3A2024%3A62%3AFIN&qid=1707312980822**, (accessed 3 April 2024).
28 A. Dubey and A. Arora, Advancements in carbon capture technologies: A review, *J. Cleaner Prod.*, 2022, **373**, 133932.
29 *Fraunhofer-Institut für Umwelt-, Sicherheits- und Energietechnik UMSICHT, Verbundprojekt Carbon2Chem® - Fraunhofer UMSICHT*, **https://www.umsicht.fraunhofer.de/de/forschungslinien/kohlenstoffkreislauf.html**, (accessed 3 April 2024).
30 W. Supronowicz, I. A. Ignatyev, G. Lolli, A. Wolf, L. Zhao and L. Mleczko, Formic acid: a future bridge between the power and chemical industries, *Green Chem.*, 2015, **17**, 2904–2911.
31 T. Galimova, M. Ram, D. Bogdanov, M. Fasihi, S. Khalili, A. Gulagi, H. Karjunen, T. N. O. Mensah and C. Breyer, Global demand analysis for carbon dioxide as raw material from key industrial sources and direct air capture to produce renewable electricity-based fuels and chemicals, *J. Cleaner Prod.*, 2022, **373**, 133920.
32 G. Lopez, T. Galimova, M. Fasihi, D. Bogdanov and C. Breyer, Towards defossilised steel: Supply chain options

for a green European steel industry, *Energy*, 2023, **273**, 127236.
33 V. Nechifor, A. Calzadilla, R. Bleischwitz, M. Winning, X. Tian and A. Usubiaga, Steel in a circular economy: Global implications of a green shift in China, *World Dev.*, 2020, **127**, 104775.
34 V. Vogl, M. Åhman and L. J. Nilsson, The making of green steel in the EU: a policy evaluation for the early commercialization phase, *Clim. Policy*, 2021, **21**, 78–92.
35 F. Xu, F. Cui and N. Xiang, Roadmap of green transformation for a steel-manufacturing intensive city in China driven by air pollution control, *J. Cleaner Prod.*, 2021, **283**, 124643.
36 M. Farghali, A. I. Osman, K. Umetsu and D. W. Rooney, Integration of biogas systems into a carbon zero and hydrogen economy: a review, *Environ. Chem. Lett.*, 2022, **20**, 2853–2927.
37 R. Lin, R. O'Shea, C. Deng, B. Wu and J. D. Murphy, A perspective on the efficacy of green gas production via integration of technologies in novel cascading circular biosystems, *Renewable Sustainable Energy Rev.*, 2021, **150**, 111427.
38 G. Lorenzi, A. Lanzini and M. Santarelli, Digester Gas Upgrading to Synthetic Natural Gas in Solid Oxide Electrolysis Cells, *Energy Fuels*, 2015, **29**, 1641–1652.
39 M. Zeppilli, D. Pavesi, M. Gottardo, F. Micolucci, M. Villano and M. Majone, Using effluents from two-phase anaerobic digestion to feed a methane-producing microbial electrolysis, *Chem. Eng. J.*, 2017, **328**, 428–433.
40 *World Population Prospects - Population Division - United Nations*, **https://population.un.org/wpp/Graphs/Probabilistic/POP/TOT/908**, (accessed 3 April 2024).
41 *Statista, EU-27: residual waste reduction target scenarios 2030 | Statista*, **https://www.statista.com/statistics/1315956/waste-reduction-target-scenarios-in-european-union/**, (accessed 3 April 2024).
42 European Commission, Joint Research CentreC. Pavel and J. Moya, *Energy efficiency and GHG emissions – Prospective scenarios for the pulp and paper industry*, Publications Office, 2018.
43 Glass For Europre, 2050 | Flat Glass in Climate-Neutral Europe 2050 | FLAT GLASS IN CLIMATE-NEUTRAL EUROPE.
44 D. Wilhelm, D. Simbeck, A. Karp and R. Dickenson, Syngas production for gas-to-liquids applications: technologies, issues and outlook, *Fuel Process. Technol.*, 2001, **71**, 139–148.
45 A. Forsyth, M. Campell and A. Robertson, Ttention all shipping methanol gains momentum industry background from longspur research.
46 *Carbon Monoxide Market Size, Share | Global Report [2032]*, **https://www.fortunebusinessinsights.com/carbon-monoxide-market-105343**, (accessed 23 March 2025).
47 *Europe Ethanol Market Size, Share, Demand & Industry Outlook By 2030*, **https://www.databridgemarketresearch.com/reports/europe-ethanol-market**, (accessed 23 March 2025).
48 Manufacturing & Construction Market Research Reports & Manufacturing & Construction Industry Analysis | **https://MarketResearch.com**, **https://www.marketresearch.com/Heavy-Industry-c1595/Manufacturing-Construction-c86/**, (accessed 23 March 2025).
49 S. Bidwai, *Formic Acid Market Size To Hit Around USD 3.78 Bn By 2034*, 2024.
50 **https://Chemanalyst.com**, *Formic Acid Market Analysis: Industry Market Size, Plant Capacity, Production, Operating Efficiency, Demand & Supply, End-User Industries, Sales Channel, Company Share, Regional Demand, Foreign Trade, 2015-2035*, **https://www.chemanalyst.com/industry-report/formic-acid-market-688**.
51 *Statista, Global formaldehyde demand share by region | Statista*, **https://www.statista.com/statistics/1323629/distribution-of-formaldehyde-demand-worldwide-by-region/**, (accessed 23 March 2025).
52 **https://Chemanalyst.com**, *Formaldehyde Market Analysis: Industry Market Size, Plant Capacity, Production, Operating Efficiency, Demand & Supply, End-User Industries, Sales Channel, Regional Demand, Foreign Trade, Company Share, Manufacturing Process, Policy and Regulatory Landscape, 2015-2032*, **https://www.chemanalyst.com/industry-report/formaldehyde-market-627**.
53 *Microsoft Research, Carbon Capture and Storage - Microsoft Research*, **https://www.microsoft.com/en-us/research/project/carbon-capture-and-storage/**, (accessed 23 March 2025).
54 M. Segal, BlackRock Invests $550 Million in World's Largest DAC Carbon Capture Project, *ESG Today*, 2023, **https://www.esgtoday.com/blackrock-invests-550-million-in-worlds-largest-dac-carbon-capture-project/**.
55 M. Göbel, *KI-Rechenzentren für das Rheinische Revier und ganz Deutschland: Microsoft stellt Pläne in NRW vor und startet Qualifizierungsoffensive*, **https://news.microsoft.com/de-de/ki-rechenzentren-fuer-das-rheinische-revier-und-ganz-deutschland-microsoft-stellt-plaene-in-nrw-vor-und-startet-qualifizierungsoffensive/**, (accessed 23 March 2025).
56 I. E. L. Stephens, K. Chan, A. Bagger, S. W. Boettcher, J. Bonin, E. Boutin, A. K. Buckley, R. Buonsanti, E. R. Cave, X. Chang, S. W. Chee, A. H. M. Da Silva, P. de Luna, O. Einsle, B. Endrődi, M. Escudero-Escribano, J. V. Ferreira de Araujo, M. C. Figueiredo, C. Hahn, K. U. Hansen, S. Haussener, S. Hunegnaw, Z. Huo, Y. J. Hwang, C. Janáky, B. S. Jayathilake, F. Jiao, Z. P. Jovanov, P. Karimi, M. T. M. Koper, K. P. Kuhl, W. H. Lee, Z. Liang, X. Liu, S. Ma, M. Ma, H.-S. Oh, M. Robert, B. R. Cuenya, J. Rossmeisl, C. Roy, M. P. Ryan, E. H. Sargent, P. Sebastián-Pascual, B. Seger, L. Steier, P. Strasser, A. S. Varela, R. E. Vos, X. Wang, B. Xu, H. Yadegari and Y. Zhou, 2022 roadmap on low temperature electrochemical CO_2 reduction, *J. Phys. Energy*, 2022, **4**, 42003.
57 V. Chanda, D. Blaudszun, L. Hoof, I. Sanjuán, K. Pellumbi, K. Junge Puring, C. Andronescu and U.-P. Apfel, Exploring the (Dis)-Similarities of Half-Cell and Full Cell Zero-Gap Electrolyzers for the CO_2 Electroreduction, *ChemElectroChem*, 2024, **11**, 202300715.

58 T. Dang, R. Ramsaran, S. Roy, J. Froehlich, J. Wang and C. P. Kubiak, Design of a High Throughput 25-Well Parallel Electrolyzer for the Accelerated Discovery of CO_2 Reduction Catalysts via a Combinatorial Approach, *Electroanalysis*, 2011, **23**, 2335–2342.
59 P. Gerschel, S. Angel, M. Hammad, A. Olean-Oliveira, B. Toplak, V. Chanda, R. Martínez-Hincapié, S. Sanden, A. R. Khan, D. Xing, A. S. Amin, H. Wiggers, H. Hoster, V. Čolić, C. Andronescu, C. Schulz, U.-P. Apfel and D. Segets, Determining materials for energy conversion across scales: The alkaline oxygen evolution reaction, *Carbon Energy*, 2024, **6**(12), e608.
60 G. Xiao, A. Sun, H. Liu, M. Ni and H. Xu, Thermal management of reversible solid oxide cells in the dynamic mode switching, *Appl. Energy*, 2023, **331**, 120383.
61 T. Haas, R. Krause, R. Weber, M. Demler and G. Schmid, Technical photosynthesis involving CO_2 electrolysis and fermentation, *Nat. Catal.*, 2018, **1**, 32–39.
62 C. Stoots, J. O'Brien and J. Hartvigsen, Results of recent high temperature coelectrolysis studies at the Idaho National Laboratory, *Int. J. Hydrogen Energy*, 2009, **34**, 4208–4215.
63 A. Hauch, R. Küngas, P. Blennow, A. B. Hansen, J. B. Hansen, B. V. Mathiesen and M. B. Mogensen, Recent advances in solid oxide cell technology for electrolysis, *Science*, 2020, **370**, eaba6118.
64 X. Zhang, Y. Song, G. Wang and X. Bao, Co-electrolysis of CO_2 and H_2O in high-temperature solid oxide electrolysis cells: Recent advance in cathodes, *J. Energy Chem.*, 2017, **26**, 839–853.
65 M. B. Mogensen, M. Chen, H. L. Frandsen, C. Graves, J. B. Hansen, K. V. Hansen, A. Hauch, T. Jacobsen, S. H. Jensen, T. L. Skafte and X. Sun, Reversible solid-oxide cells for clean and sustainable energy, *Clean Energy*, 2019, **3**, 175–201.
66 S. E. Wolf, F. E. Winterhalder, V. Vibhu, L. G. J. de Haart, O. Guillon, R.-A. Eichel and N. H. Menzler, Solid oxide electrolysis cells – current material development and industrial application, *J. Mater. Chem. A*, 2023, **11**, 17977–18028.
67 H. Seo, S. Jang, W. Lee, K. Taek Bae, K. Taek Lee, J. Hong and K. Joong Yoon, Highly efficient, coke-free electrolysis of dry CO_2 in solid oxide electrolysis cells, *Chem. Eng. J.*, 2024, **481**, 148532.
68 M. Torrell, S. García-Rodríguez, A. Morata, G. Penelas and A. Tarancón, Co-electrolysis of steam and CO_2 in full-ceramic symmetrical SOECs: a strategy for avoiding the use of hydrogen as a safe gas, *Faraday Discuss.*, 2015, **182**, 241–255.
69 Y. Zheng, J. Wang, B. Yu, W. Zhang, J. Chen, J. Qiao and J. Zhang, A review of high temperature co-electrolysis of H_2O and CO_2 to produce sustainable fuels using solid oxide electrolysis cells (SOECs): advanced materials and technology, *Chem. Soc. Rev.*, 2017, **46**, 1427–1463.
70 M. F. Rabuni, N. Vatcharasuwan, T. Li and K. Li, High performance micro-monolithic reversible solid oxide electrochemical reactor, *J. Power Sources*, 2020, **458**, 228026.
71 B. Endrődi, E. Kecsenovity, A. Samu, T. Halmágyi, S. Rojas-Carbonell, L. Wang, Y. Yan and C. Janáky, High carbonate ion conductance of a robust PiperION membrane allows industrial current density and conversion in a zero-gap carbon dioxide electrolyzer cell, *Energy Environ. Sci.*, 2020, **13**, 4098–4105.
72 A. Senocrate, F. Bernasconi, P. Kraus, N. Plainpan, J. Trafkowski, F. Tolle, T. Weber, U. Sauter and C. Battaglia, Parallel experiments in electrochemical CO_2 reduction enabled by standardized analytics, *Nat. Catal.*, 2024, **7**, 742–752.
73 A. Loh, X. Li, S. Sluijter, P. Shirvanian, Q. Lai and Y. Liang, Design and Scale-Up of Zero-Gap AEM Water Electrolysers for Hydrogen Production, *Hydrogen*, 2023, **4**, 257–271.
74 E. W. Lees, M. Goldman, A. G. Fink, D. J. Dvorak, D. A. Salvatore, Z. Zhang, N. W. X. Loo and C. P. Berlinguette, Electrodes Designed for Converting Bicarbonate into CO, *ACS Energy Lett.*, 2020, **5**, 2165–2173.
75 M. E. Leonard, M. J. Orella, N. Aiello, Y. Román-Leshkov, A. Forner-Cuenca and F. R. Brushett, Editors' Choice—Flooded by Success: On the Role of Electrode Wettability in CO_2 Electrolyzers that Generate Liquid Products, *J. Electrochem. Soc.*, 2020, **167**, 124521.
76 Y. Wu, H. Rabiee, X. S. Zhao, G. Wang and Y. Jiang, Insights into electrolyte flooding in flexible gas diffusion electrodes for CO_2 electrolysis: from mechanisms to effective mitigation strategies, *J. Mater. Chem. A*, 2024, **12**, 14206–14228.
77 C. Delacourt, P. L. Ridgway, J. B. Kerr and J. Newman, Design of an Electrochemical Cell Making Syngas (CO + H[sub 2]) from CO[sub 2] and H[sub 2]O Reduction at Room Temperature, *J. Electrochem. Soc.*, 2008, **155**, B42.
78 D. T. Whipple, E. C. Finke and P. J. A. Kenis, Microfluidic Reactor for the Electrochemical Reduction of Carbon Dioxide: The Effect of pH, *Electrochem. Solid-State Lett.*, 2010, **13**, B109.
79 H. M. Almajed, O. J. Guerra, W. A. Smith, B.-M. Hodge and A. Somoza-Tornos, Evaluating the techno-economic potential of defossilized air-to-syngas pathways, *Energy Environ. Sci.*, 2023, **16**, 6127–6146.
80 M. Moreno-Gonzalez, A. Berger, T. Borsboom-Hanson and W. Mérida, Carbon-neutral fuels and chemicals: Economic analysis of renewable syngas pathways via CO_2 electrolysis, *Energy Convers. Manage.*, 2021, **244**, 114452.
81 S. Guo, T. Asset and P. Atanassov, Catalytic Hybrid Electrocatalytic/Biocatalytic Cascades for Carbon Dioxide Reduction and Valorization, *ACS Catal.*, 2021, **11**, 5172–5188.
82 M. Jouny, G. S. Hutchings and F. Jiao, Carbon monoxide electroreduction as an emerging platform for carbon utilization, *Nat. Catal.*, 2019, **2**, 1062–1070.
83 M. G. Lee, X.-Y. Li, A. Ozden, J. Wicks, P. Ou, Y. Li, R. Dorakhan, J. Lee, H. K. Park, J. W. Yang, B. Chen, J. Abed, R. dos Reis, G. Lee, J. E. Huang, T. Peng, Y.-H. Chin, D. Sinton and E. H. Sargent, Selective synthesis of butane from carbon monoxide using cascade electrolysis and thermocatalysis at ambient conditions, *Nat. Catal.*, 2023, **6**, 310–318.

84 A. Ozden, F. P. García de Arquer, J. E. Huang, J. Wicks, J. Sisler, R. K. Miao, C. P. O'Brien, G. Lee, X. Wang, A. H. Ip, E. H. Sargent and D. Sinton, Carbon-efficient carbon dioxide electrolysers, *Nat. Sustain.*, 2022, **5**, 563–573.

85 R. Küngas, Review—Electrochemical CO_2 Reduction for CO Production: Comparison of Low- and High-Temperature Electrolysis Technologies, *J. Electrochem. Soc.*, 2020, **167**(4), 44508.

86 S. Rashidi, N. Karimi, B. Sunden, K. C. Kim, A. G. Olabi and O. Mahian, Progress and challenges on the thermal management of electrochemical energy conversion and storage technologies: Fuel cells, electrolysers, and supercapacitors, *Prog. Energy Combust. Sci.*, 2022, **88**, 100966.

87 A. L. Dipu, Y. Ujisawa, J. Ryu and Y. Kato, Carbon dioxide reduction in a tubular solid oxide electrolysis cell for a carbon recycling energy system, *Nucl. Eng. Des.*, 2014, **271**, 30–35.

88 A. L. Dipu, Y. Ujisawa, J. Ryu and Y. Kato, Electrolysis of carbon dioxide for carbon monoxide production in a tubular solid oxide electrolysis cell, *Ann. Nucl. Energy*, 2015, **81**, 257–262.

89 G. Kaur, A. P. Kulkarni, D. Fini, S. Giddey and A. Seeber, High-performance composite cathode for electrolysis of CO_2 in tubular solid oxide electrolysis cells: A pathway for efficient CO_2 utilization, *J. CO_2* Util., 2020, **41**, 101271.

90 G. Kaur, A. P. Kulkarni and S. Giddey, CO_2 reduction in a solid oxide electrolysis cell with a ceramic composite cathode: Effect of load and thermal cycling, *Int. J. Hydrogen Energy*, 2018, **43**, 21769–21776.

91 G. Kaur, A. P. Kulkarni, S. Giddey and S. P. Badwal, Ceramic composite cathodes for CO_2 conversion to CO in solid oxide electrolysis cells, *Appl. Energy*, 2018, **221**, 131–138.

92 S.-B. Yu, S.-H. Lee, M. T. Mehran, J.-E. Hong, J.-W. Lee, S.-B. Lee, S.-J. Park, R.-H. Song, J.-H. Shim, Y.-G. Shul and T.-H. Lim, Syngas production in high performing tubular solid oxide cells by using high-temperature H_2O/CO_2 co-electrolysis, *Chem. Eng. J.*, 2018, **335**, 41–51.

93 Y. Xie, J. Xiao, D. Liu, J. Liu and C. Yang, Electrolysis of Carbon Dioxide in a Solid Oxide Electrolyzer with Silver-Gadolinium-Doped Ceria Cathode, *J. Electrochem. Soc.*, 2015, **162**, F397–F402.

94 X. Li, Y. Wang, W. Liu, J. A. Wilson, J. Wang, C. Wang, J. Yang, C. Xia, X.-D. Zhou and W. Guan, Reliability of CO_2 electrolysis by solid oxide electrolysis cells with a flat tube based on a composite double-sided air electrode, *Composites, Part B*, 2019, **166**, 549–554.

95 A. Wu, B. Han, Y. Yao, Y. Zhang, Y. Tang, S. Hanson, J. Wang, W. Guan and S. C. Singhal, Degradation of flat-tube solid oxide electrolytic stack for co-electrolysis of H_2O and CO_2 under pulsed current, *J. Power Sources*, 2023, **580**, 233372.

96 A. Wu, C. Li, B. Han, W. Liu, Y. Zhang, S. Hanson, W. Guan and S. C. Singhal, Pulsed electrolysis of carbon dioxide by large-scale solid oxide electrolytic cells for intermittent renewable energy storage, *Carbon Energy*, 2023, **5**(4), e262.

97 C. Xi, J. Sang, A. Wu, J. Yang, X. Qi, W. Guan, J. Wang and S. C. Singhal, Electrochemical performance and durability of flat-tube solid oxide electrolysis cells for H_2O/CO_2 co-electrolysis, *Int. J. Hydrogen Energy*, 2022, **47**, 10166–10174.

98 D.-Y. Lee, M. T. Mehran, J. Kim, S. Kim, S.-B. Lee, R.-H. Song, E.-Y. Ko, J.-E. Hong, J.-Y. Huh and T.-H. Lim, Scaling up syngas production with controllable H_2/CO ratio in a highly efficient, compact, and durable solid oxide coelectrolysis cell unit-bundle, *Appl. Energy*, 2020, **257**, 114036.

99 L. Lu, W. Liu, J. Wang, Y. Wang, C. Xia, X.-D. Zhou, M. Chen and W. Guan, Long-term stability of carbon dioxide electrolysis in a large-scale flat-tube solid oxide electrolysis cell based on double-sided air electrodes, *Appl. Energy*, 2020, **259**, 114130.

100 X. Hou, Y. Jiang, K. Wei, C. Jiang, T.-C. Jen, Y. Yao, X. Liu, J. Ma and J. T. S. Irvine, Syngas Production from CO_2 and H_2O via Solid-Oxide Electrolyzer Cells: Fundamentals, Materials, Degradation, Operating Conditions, and Applications, *Chem. Rev.*, 2024, **124**, 5119–5166.

101 L. A. Jolaoso, I. T. Bello, O. A. Ojelade, A. Yousuf, C. Duan and P. Kazempoor, Operational and scaling-up barriers of SOEC and mitigation strategies to boost H2 production- a comprehensive review, *Int. J. Hydrogen Energy*, 2023, **48**, 33017–33041.

102 Y. C. Xiao, C. M. Gabardo, S. Liu, G. Lee, Y. Zhao, C. P. O'Brien, R. K. Miao, Y. Xu, J. P. Edwards, M. Fan, J. E. Huang, J. Li, P. Papangelakis, T. Alkayyali, A. Sedighian Rasouli, J. Zhang, E. H. Sargent and D. Sinton, Direct carbonate electrolysis into pure syngas, *EES. Catal.*, 2023, **1**, 54–61.

103 G. Leverick, E. M. Bernhardt, A. I. Ismail, J. H. Law, A. Arifutzzaman, M. K. Aroua and B. M. Gallant, Uncovering the Active Species in Amine-Mediated CO_2 Reduction to CO on Ag, *ACS Catal.*, 2023, **13**, 12322–12337.

104 T. Li, E. W. Lees, M. Goldman, D. A. Salvatore, D. M. Weekes and C. P. Berlinguette, Electrolytic Conversion of Bicarbonate into CO in a Flow Cell, *Joule*, 2019, **3**, 1487–1497.

105 B. Belsa, L. Xia and F. P. García de Arquer, CO_2 Electrolysis Technologies: Bridging the Gap toward Scale-up and Commercialization, *ACS Energy Lett.*, 2024, **9**, 4293–4305.

106 A. Raya-Imbernón, A. A. Samu, S. Barwe, G. Cusati, T. Fődi, B. M. Hepp and C. Janáky, Renewable Syngas Generation via Low-Temperature Electrolysis: Opportunities and Challenges, *ACS Energy Lett.*, 2024, **9**, 288–297.

107 H.-P. van Iglesias Montfort, S. Subramanian, E. Irtem, M. Sassenburg, M. Li, J. Kok, J. Middelkoop and T. Burdyny, An Advanced Guide to Assembly and Operation of CO_2 Electrolyzers, *ACS Energy Lett.*, 2023, **8**, 4156–4161.

108 H. Song, C. A. Fernández, H. Choi, P.-W. Huang, J. Oh and M. C. Hatzell, Integrated carbon capture and CO production from bicarbonates through bipolar membrane electrolysis, *Energy Environ. Sci.*, 2024, **17**, 3570–3579.

109 R. B. Kutz, Q. Chen, H. Yang, S. D. Sajjad, Z. Liu and I. R. Masel, Sustainion Imidazolium-Functionalized Polymers for Carbon Dioxide Electrolysis, *Energy Tech.*, 2017, **5**, 929–936.

110 R. Krause, D. Reinisch, C. Reller, H. Eckert, D. Hartmann, D. Taroata, K. Wiesner-Fleischer, A. Bulan, A. Lueken and

G. Schmid, Industrial Application Aspects of the Electrochemical Reduction of CO_2 to CO in Aqueous Electrolyte, *Chem. Ing. Tech.*, 2020, **92**, 53–61.

111 J. Disch, L. Bohn, L. Metzler and S. Vierrath, Strategies for the mitigation of salt precipitation in zero-gap CO_2 electrolyzers producing CO, *J. Mater. Chem. A*, 2023, **11**, 7344–7357.

112 C. Martens, B. Schmid, H. Tempel and R.-A. Eichel, CO_2 flow electrolysis – limiting impact of heat and gas evolution in the electrolyte gap on current density, *Green Chem.*, 2023, **25**, 7794–7806.

113 D. Segets, C. Andronescu and U.-P. Apfel, Accelerating CO_2 electrochemical conversion towards industrial implementation, *Nat. Commun.*, 2023, **14**, 7950.

114 A. Löwe, M. Schmidt, F. Bienen, D. Kopljar, N. Wagner and E. Klemm, Optimizing Reaction Conditions and Gas Diffusion Electrodes Applied in the CO_2 Reduction Reaction to Formate to Reach Current Densities up to 1.8 A cm^{-2}, *ACS Sustainable Chem. Eng.*, 2021, **9**, 4213–4223.

115 X.-D. Liang, Q.-Z. Zheng, N. Wei, Y.-Y. Lou, S.-N. Hu, K.-M. Zhao, H.-G. Liao, N. Tian, Z.-Y. Zhou and S.-G. Sun, In-situ constructing $Bi@Bi_2O_2CO_3$ nanosheet catalyst for ampere-level CO_2 electroreduction to formate, *Nano Energy*, 2023, **114**, 108638.

116 Z. Xing, X. Hu and X. Feng, Tuning the Microenvironment in Gas-Diffusion Electrodes Enables High-Rate CO_2 Electrolysis to Formate, *ACS Energy Lett.*, 2021, **6**, 1694–1702.

117 Z. Wang, Y. Zhou, C. Xia, W. Guo, B. You and B. Y. Xia, Efficient Electroconversion of Carbon Dioxide to Formate by a Reconstructed Amino-Functionalized Indium-Organic Framework Electrocatalyst, *Angew. Chem., Int. Ed.*, 2021, **60**, 19107–19112.

118 Z. Chen, D. Zhang, Y. Zhao, D. Jia, H. Zhang, L. Liu and X. He, Indium oxide induced electron-deficient indium hollow nanotubes for stable electroreduction of CO_2 at industrial current densities, *Chem. Eng. J.*, 2023, **464**, 142573.

119 Y. Qi, Q. Dong, L. Zhong, Z. Liu, P. Qiu, R. Cheng, X. He, J. Vanderbilt and B. Liu, Role of 1,2-Dimethoxyethane in the Transformation from Ethylene Polymerization to Trimerization Using Chromium Tris(2-ethylhexanoate)-Based Catalyst System: A DFT Study, *Organometallics*, 2010, **29**, 1588–1602.

120 A. Goller, J. Obenauf, W. P. Kretschmer and R. Kempe, The Highly Controlled and Efficient Polymerization of Ethylene, *Angew. Chem., Int. Ed.*, 2023, **62**, e202216464.

121 R. Beucher, C. Cammarano, E. Rodríguez-Castellón and V. Hulea, Direct Transformation of Ethylene to Propylene by Cascade Catalytic Reactions under Very Mild Conditions, *Ind. Eng. Chem. Res.*, 2020, **59**, 7438–7446.

122 B. Belsa, L. Xia, V. Golovanova, B. Polesso, A. Pinilla-Sánchez, L. San Martín, J. Ye, C.-T. Dinh and F. P. García de Arquer, Materials challenges on the path to gigatonne CO_2 electrolysis, *Nat. Rev. Mater.*, 2024, **9**, 535–549.

123 M. Li, Y. Hu, T. Wu, A. Sumboja and D. Geng, How to enhance the C_2 products selectivity of copper-based catalysts towards electrochemical CO_2 reduction? —A review, *Mater. Today*, 2023, **67**, 320–343.

124 J. Ding, H. Bin Yang, X.-L. Ma, S. Liu, W. Liu, Q. Mao, Y. Huang, J. Li, T. Zhang and B. Liu, A tin-based tandem electrocatalyst for CO_2 reduction to ethanol with 80% selectivity, *Nat. Energy*, 2023, **8**, 1386–1394.

125 Y. Song, R. Peng, D. K. Hensley, P. V. Bonnesen, L. Liang, Z. Wu, H. M. Meyer, M. Chi, C. Ma, B. G. Sumpter and A. J. Rondinone, High-Selectivity Electrochemical Conversion of CO_2 to Ethanol using a Copper Nanoparticle/N-Doped Graphene Electrode, *ChemistrySelect*, 2016, **1**, 6055–6061.

126 C. Guo, Y. Guo, Y. Shi, X. Lan, Y. Wang, Y. Yu and B. Zhang, Electrocatalytic Reduction of CO_2 to Ethanol at Close to Theoretical Potential via Engineering Abundant Electron-Donating $Cu\delta^+$ Species, *Angew. Chem.*, 2022, **61**(32), 1–5.

127 Y. Hu, J. Zhu, X. Wang, X. Zheng, X. Zhang, C. Wu, J. Zhang, C. Fu, T. Sheng and Z. Wu, Mo^{4+}-Doped CuS Nanosheet-Assembled Hollow Spheres for CO_2 Electroreduction to Ethanol in a Flow Cell, *Inorg. Chem.*, 2024, **63**, 9983–9991.

128 W. Ma, S. Xie, T. Liu, Q. Fan, J. Ye, F. Sun, Z. Jiang, Q. Zhang, J. Cheng and Y. Wang, Electrocatalytic reduction of CO_2 to ethylene and ethanol through hydrogen-assisted C–C coupling over fluorine-modified copper, *Nat. Catal.*, 2020, **3**, 478–487.

129 M. Fang, M. Wang, Z. Wang, Z. Zhang, H. Zhou, L. Dai, Y. Zhu and L. Jiang, Hydrophobic, Ultrastable Cuδ+ for Robust CO_2 Electroreduction to C_2 Products at Ampere-Current Levels, *J. Am. Chem. Soc.*, 2023, **145**, 11323–11332.

130 R. K. Miao, Y. Xu, A. Ozden, A. Robb, C. P. O'Brien, C. M. Gabardo, G. Lee, J. P. Edwards, J. E. Huang, M. Fan, X. Wang, S. Liu, Y. Yan, E. H. Sargent and D. Sinton, Electroosmotic flow steers neutral products and enables concentrated ethanol electroproduction from CO_2, *Joule*, 2021, **5**, 2742–2753.

131 H.-L. Zhu, J.-R. Huang, M.-D. Zhang, C. Yu, P.-Q. Liao and X.-M. Chen, Continuously Producing Highly Concentrated and Pure Acetic Acid Aqueous Solution via Direct Electroreduction of CO_2, *J. Am. Chem. Soc.*, 2024, **146**, 1144–1152.

132 *Covestro strengthens sustainability and competitiveness of TDI production*, Covestro, 2023.

133 G. Castelan, *Eco-profile of toluene diisocyanate (TDI) and methylene diphenyl diisocyanate (MDI)*.

134 A. van Tuyll, L. Graamans and A. Boedijn, *Carbon dioxide enrichment in a decarbonised future*, Wageningen Plant Research, Bleiswijk, 2022, **https://edepot.wur.nl/582215**.

135 S. Rokade, *Potassium Formate Market Sales to Top USD 1049.0 Mn by 2033*, Market Herald, 2025.

136 J. Eppinger and K.-W. Huang, Formic Acid as a Hydrogen Energy Carrier, *ACS Energy Lett.*, 2017, **2**, 188–195.

137 A. A. Samu, A. Kormányos, E. Kecsenovity, N. Szilágyi, B. Endrődi and C. Janáky, Intermittent Operation of CO_2 Electrolyzers at Industrially Relevant Current Densities, *ACS Energy Lett.*, 2022, **7**, 1859–1861.